Three-body forces: From exotic nuclei to neutron stars

Achim Schwenk

TECHNISCHE UNIVERSITÄT DARMSTADT

EMMI

Szymański Prize

Un Warsaw, Nov. 7, 2013

ARCHES

Award for Research Cooperation and High Excellence in Science

Bundesministerium für Bildung und Forschung


Nagroda imienia
Zdzisława Szymańskiego

Three-body forces: From exotic nuclei to neutron stars

Achim Schwenk

TECHNISCHE UNIVERSITÄT DARMSTADT

EMMI

Szymański Prize

Un… Warsaw, Nov. 7, 2015

S-DALINAC

DFG

erc

HELMHOLTZ ASSOCIATION

Minerva Stiftung

ARCHES
Award for Research Cooperation and High Excellence in Science

Bundesministerium für Bildung und Forschung

Outline

Understanding three-nucleon (3N) forces

3N forces and neutron-rich nuclei

3N forces and neutron matter/stars

Dark matter response of nuclei

Why are there three-body forces?

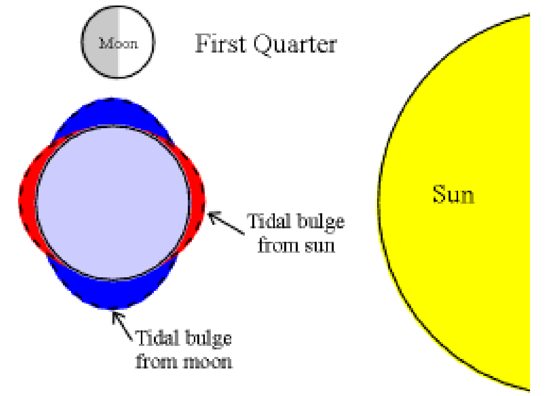

tidal effects lead to 3-body forces
in earth-sun-moon system

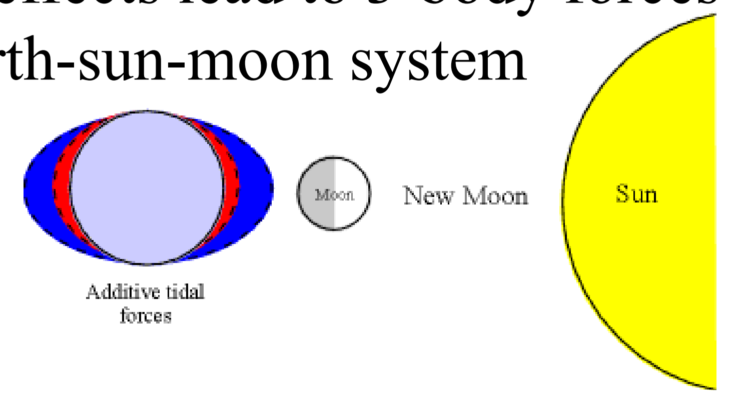

Why are there 3N forces?

Nucleons are finite-mass composite particles,
can be excited to resonances

dominant contribution from Δ(1232 MeV)

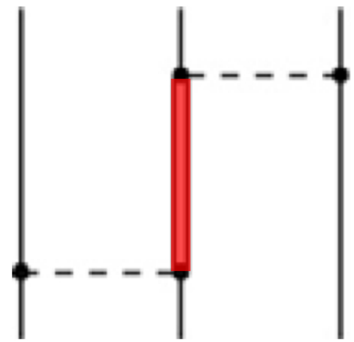

+ many shorter-range parts

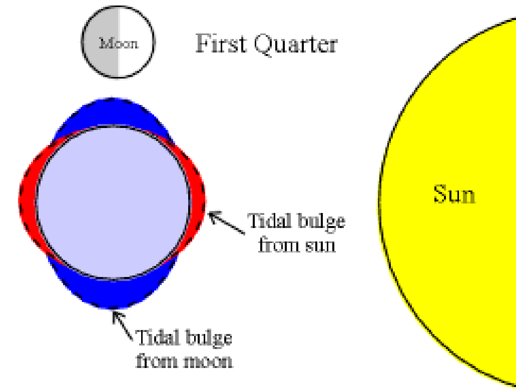

tidal effects lead to 3-body forces
in earth-sun-moon system

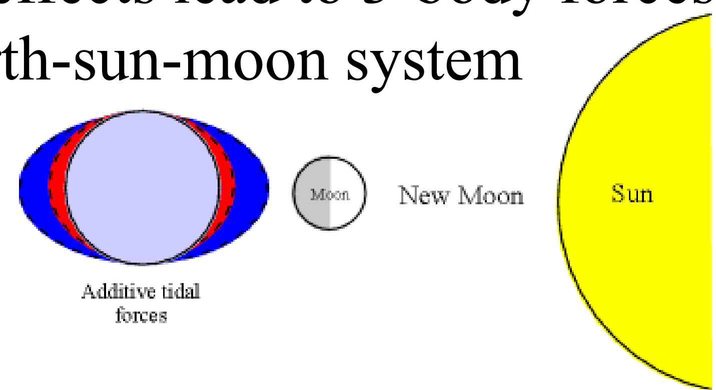

chiral effective field theory (EFT)
Delta-less (Δ is treated as heavy):

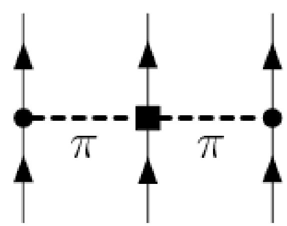

horter-range parts

EFT provides a systematic and powerful approach for 3N forces

Chiral effective field theory for nuclear forces

Separation of scales: low momenta $\frac{1}{\lambda} = Q \ll \Lambda_b$ breakdown scale ~500 MeV

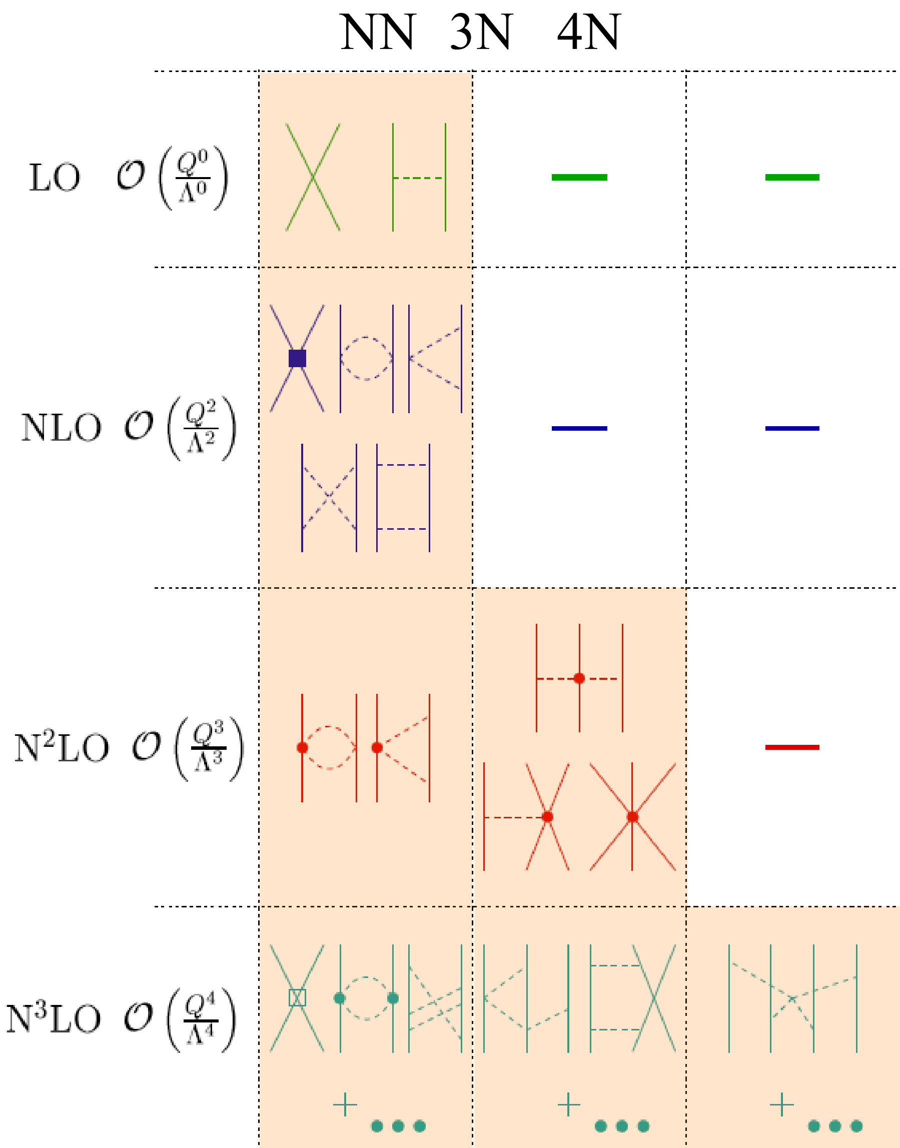

limited resolution at low energies, can expand in powers (Q/Λb)n

LO, n=0 - leading order,
NLO, n=2 - next-to-leading order,…

expansion parameter ~ 1/3

(compare to multipole expansion for a charge distribution)

Weinberg, van Kolck, Kaplan, Savage, Wise, Bernard, Epelbaum, Kaiser, Machleidt, Meissner,…

Chiral effective field theory for nuclear forces

Separation of scales: low momenta $\frac{1}{\lambda} = Q \ll \Lambda_b$ breakdown scale ~500 MeV

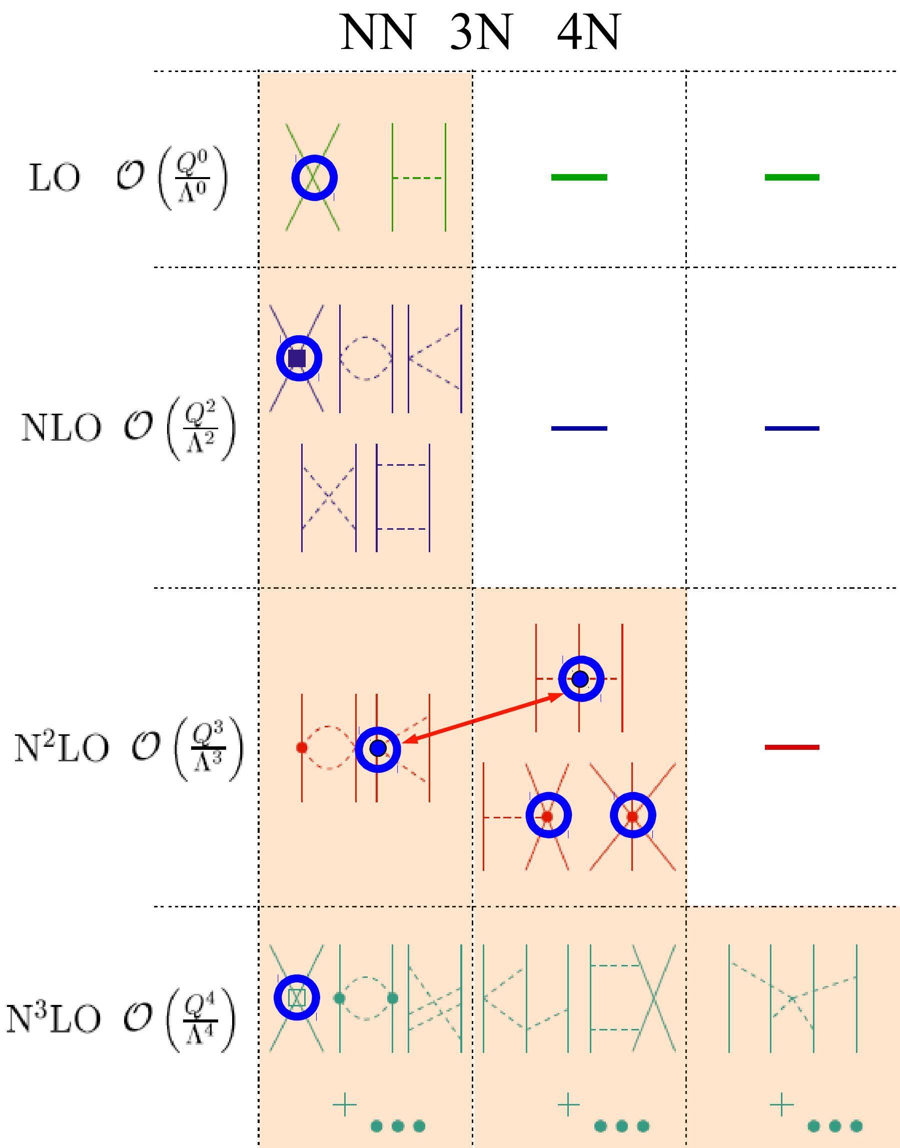

include long-range pion physics

few short-range couplings,
fit to experiment once

systematic: can work to desired accuracy and obtain **error estimates**

consistent **electroweak interactions** and **matching to lattice QCD**

Weinberg, van Kolck, Kaplan, Savage, Wise, Bernard, Epelbaum, Kaiser, Machleidt, Meissner,…

Chiral effective field theory and **many-body forces**

Separation of scales: low momenta $\frac{1}{\lambda} = Q \ll \Lambda_b$ breakdown scale ~500 MeV

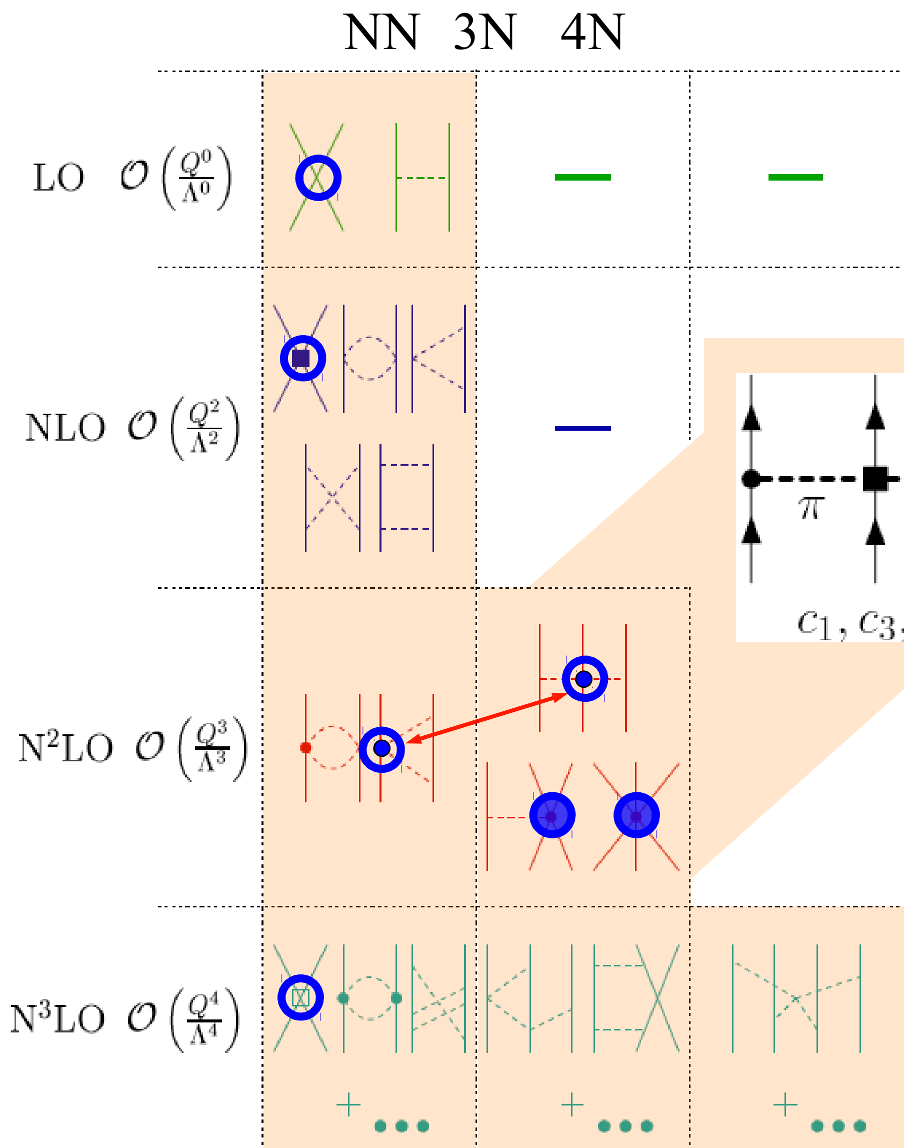

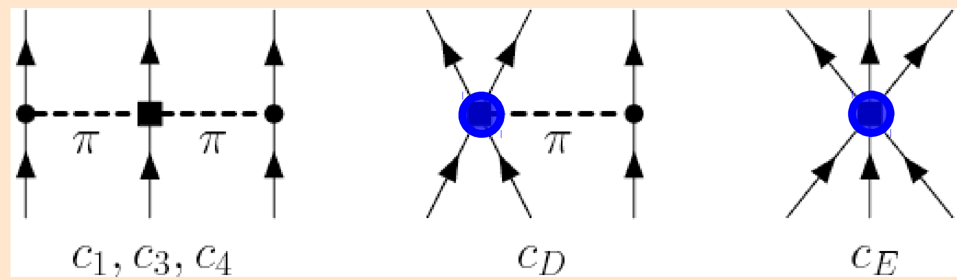

consistent NN-3N-4N interactions

3N,4N: **2 new couplings to N3LO**

ci from πN and NN Meissner et al. (2007)

$$c_1 = -0.9^{+0.2}_{-0.5}\,,\quad c_3 = -4.7^{+1.2}_{-1.0}\,,\quad c_4 = 3.5^{+0.5}_{-0.2}$$

single-Δ: c1=0, c3=-c4/2=-3 GeV-1

cD, cE fit to 3H, 4He properties only

Weinberg, van Kolck, Kaplan, Savage, Wise, Bernard, Epelbaum, Kaiser, Machleidt, Meissner,…

The oxygen anomaly

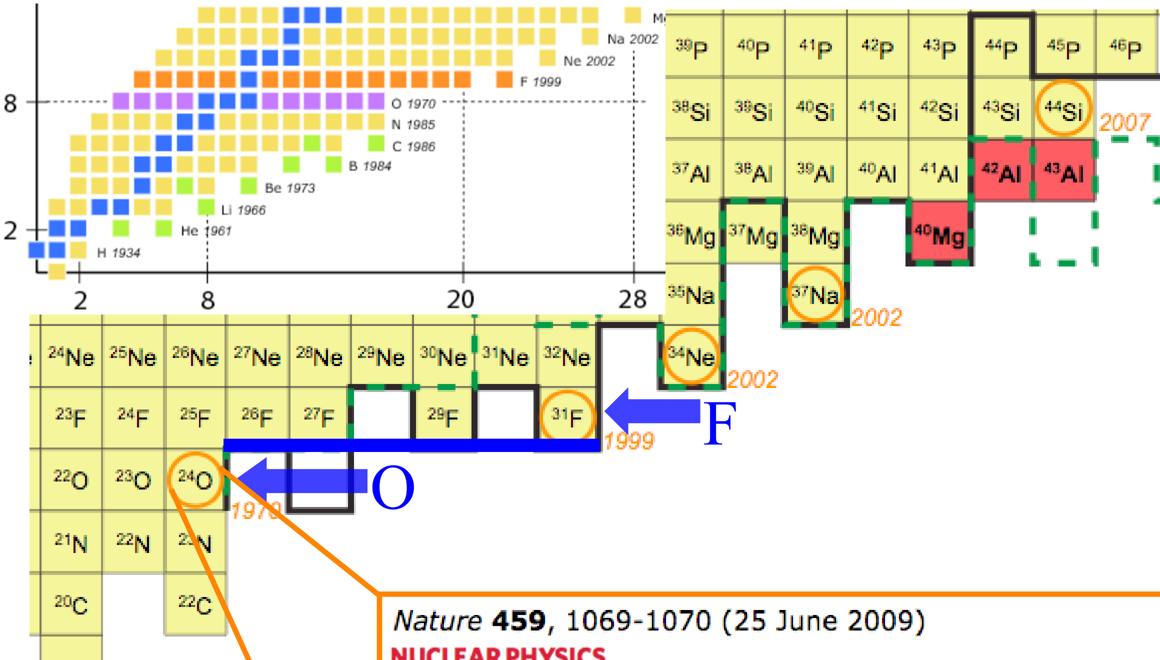

Nature **459**, 1069-1070 (25 June 2009)

NUCLEAR PHYSICS

Unexpected doubly magic nucleus

Robert V. F. Janssens

Nuclei with a ‘magic’ number of both protons and neutrons, dubbed doubly magic, are particularly stable. The oxygen isotope ^{24}O has been found to be one such nucleus — yet it lies just at the limit of stability.

The oxygen anomaly - not reproduced without 3N forces

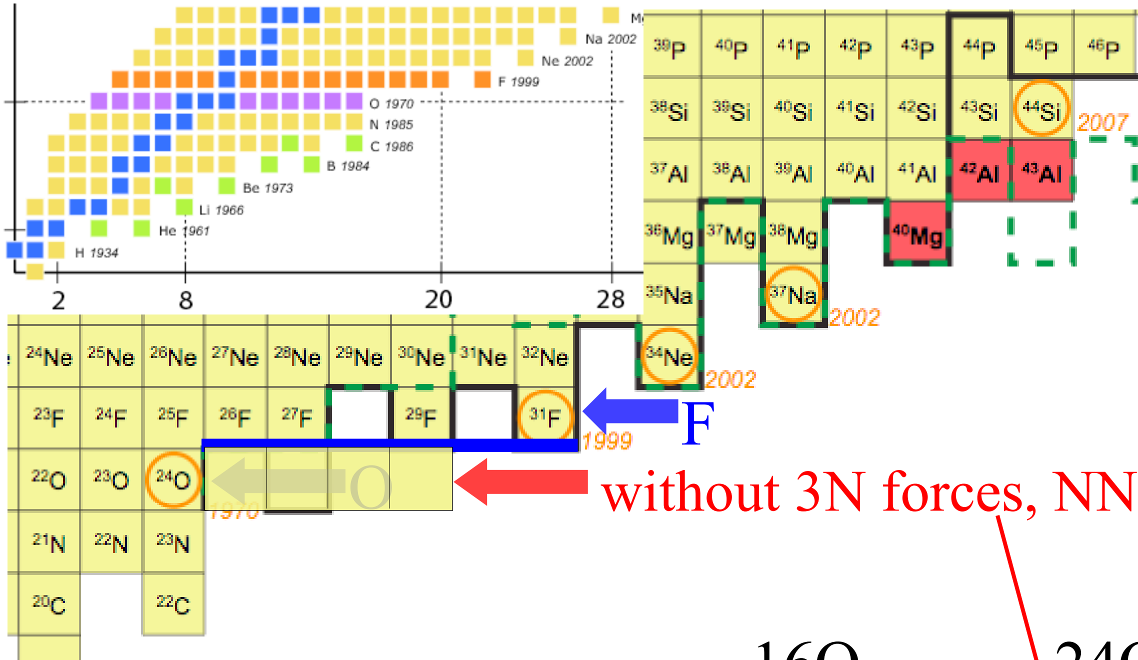

without 3N forces, NN interactions too attractive

many-body theory based on two-nucleon forces:
drip-line incorrect at 28O

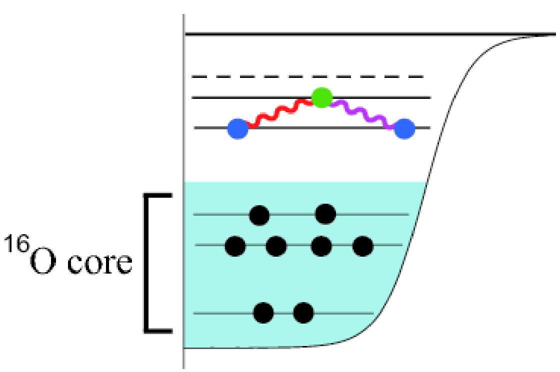

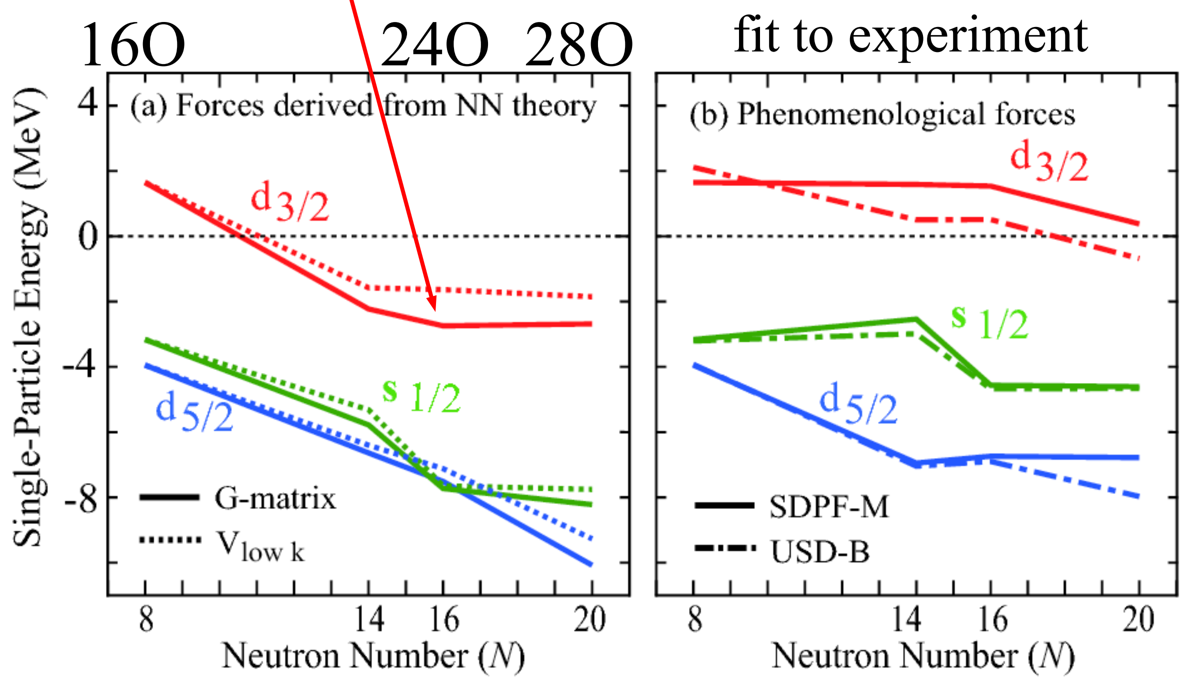

The shell model - impact of 3N forces

include ‘normal-ordered’ 2-body part of 3N forces (enhanced by core A)

leads to repulsive interactions between valence neutrons

contributions from residual three valence-nucleon interactions suppressed by Eex/EF ~ Nvalence/Ncore

Friman, AS (2011)

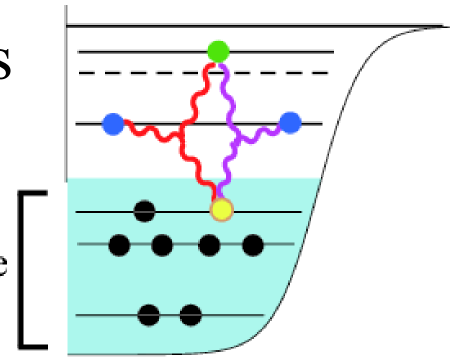

Oxygen isotopes - impact of 3N forces

include ‘normal-ordered’ 2-body part of 3N forces (enhanced by core A)

leads to repulsive interactions between valence neutrons

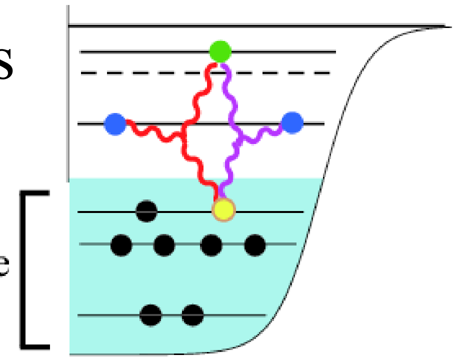

contributions from residual three valence-nucleon interactions suppressed by Eex/EF ~ Nvalence/Ncore

Friman, AS (2011)

d3/2 orbital remains unbound from 16O to 28O

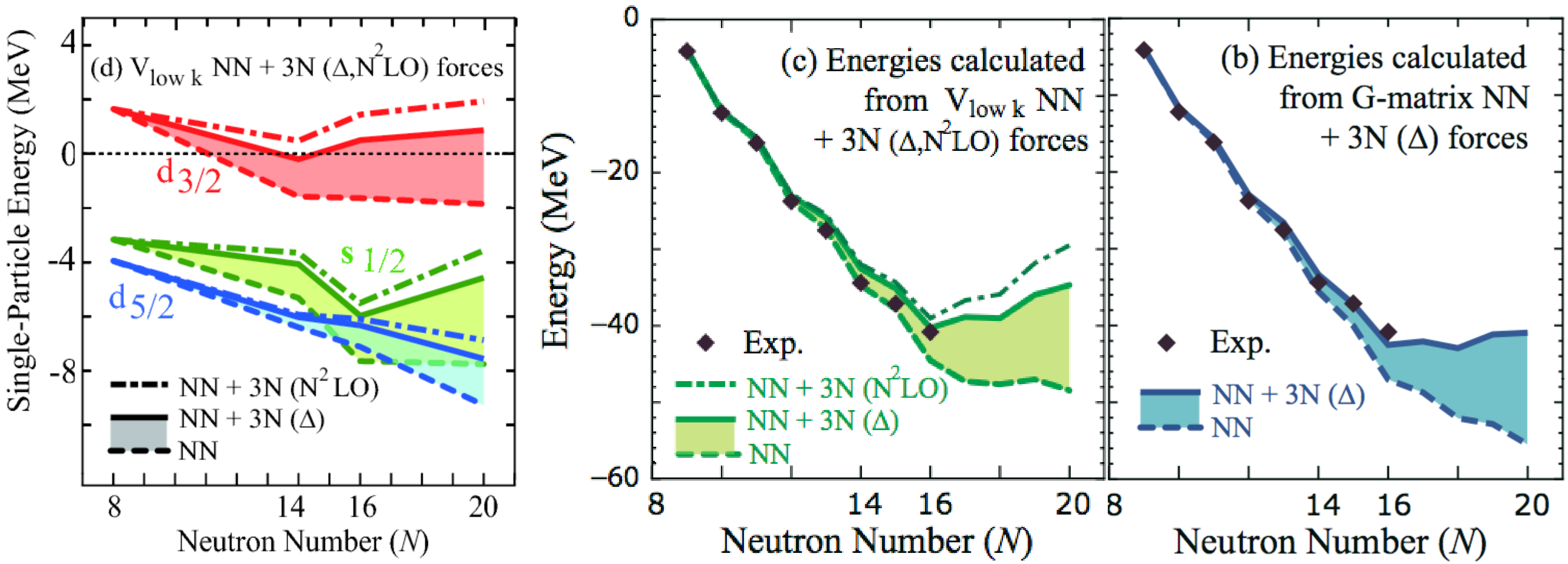

microscopic explanation of the oxygen anomaly Otsuka et al. (2010)

New ab-initio methods extend reach

impact of 3N forces confirmed in large-space calculations:

Coupled Cluster theory with phenomenological 3N forces Hagen et al. (2012)

In-Medium Similarity RG based on chiral NN+3N Hergert et al. (2013)

Green's function methods based on chiral NN+3N Cipollone et al. (2013)

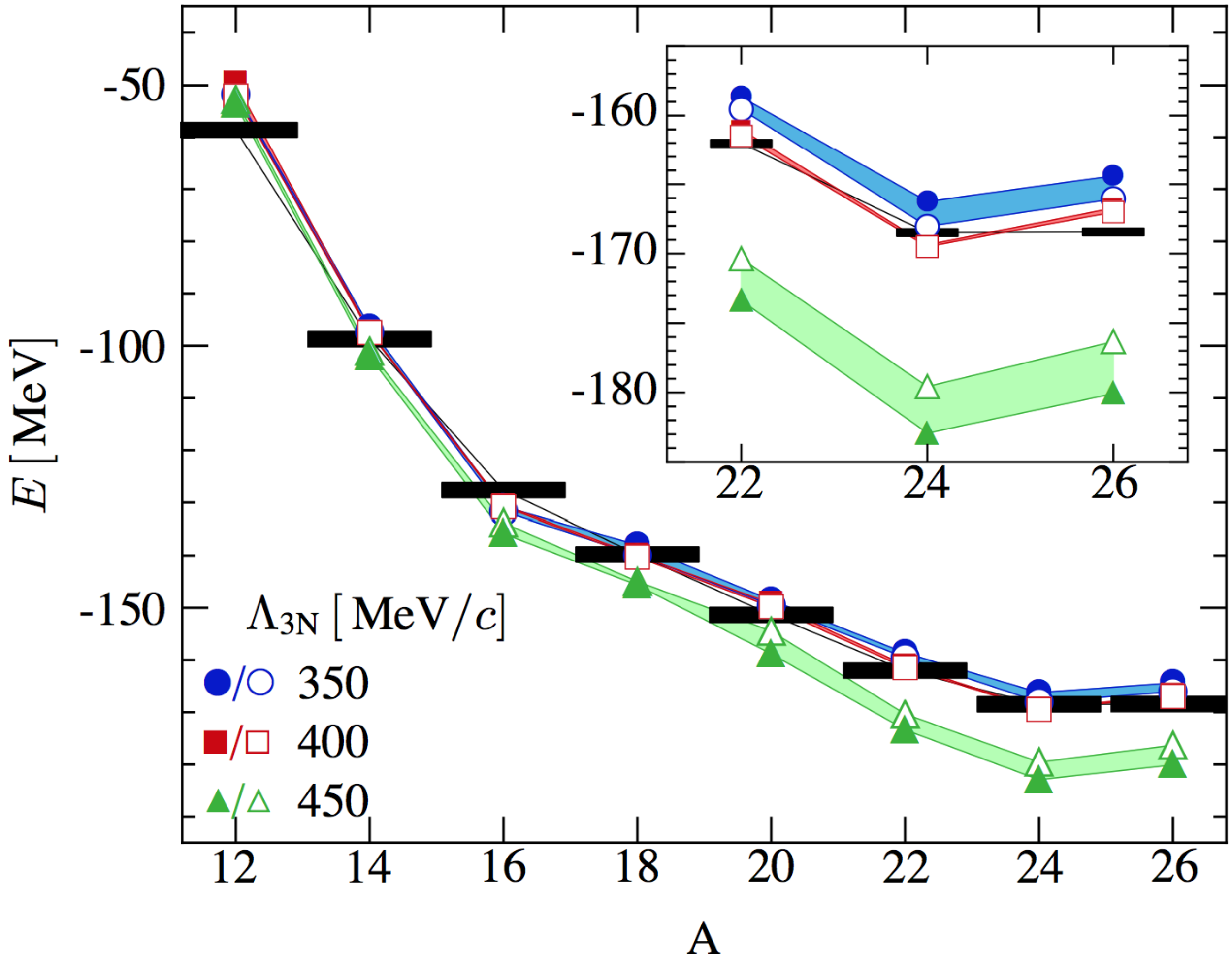

Three-body forces and magic numbers

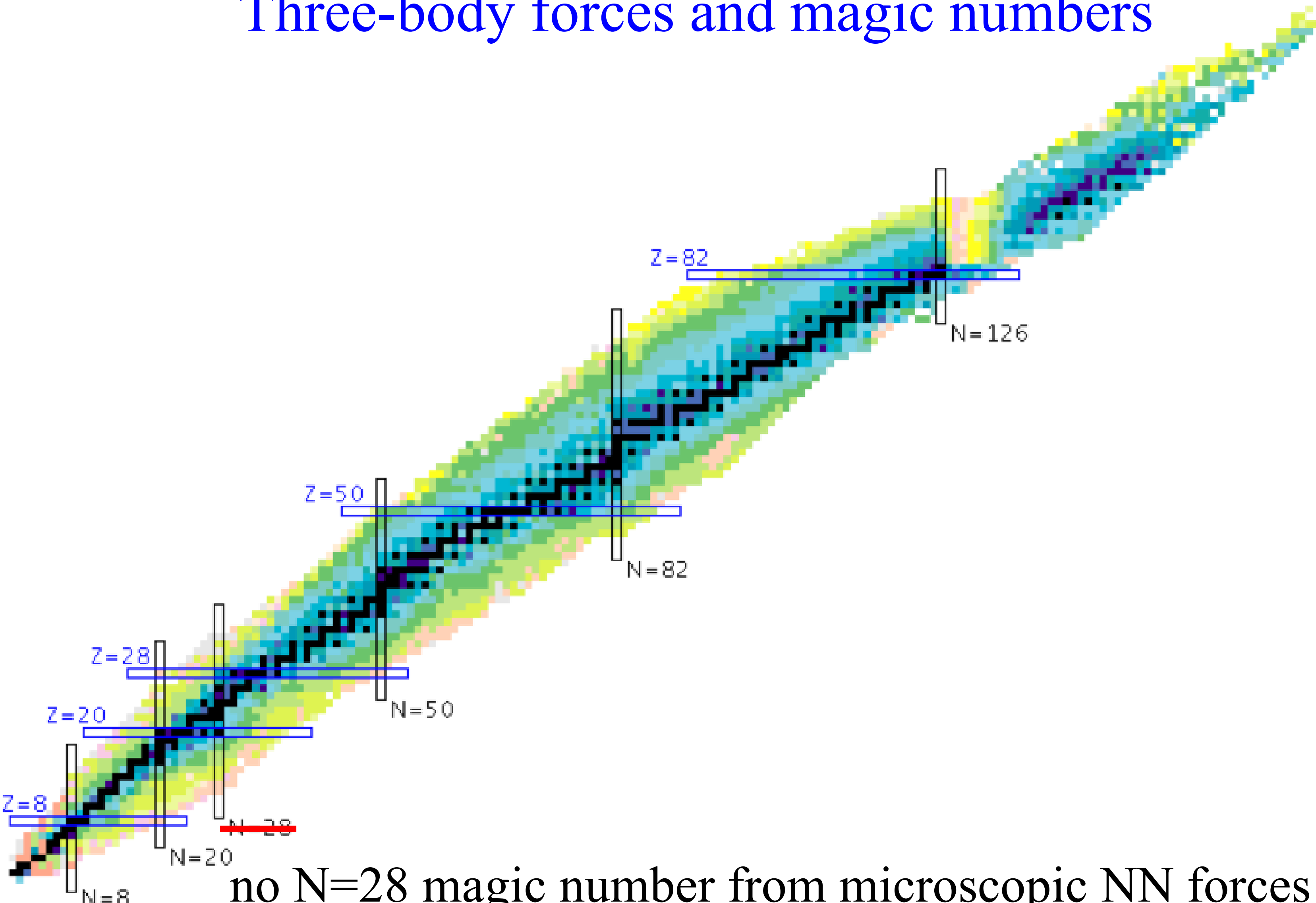

no N=28 magic number from microscopic NN forces

Zuker, Poves,…

Three-body forces and magic numbers

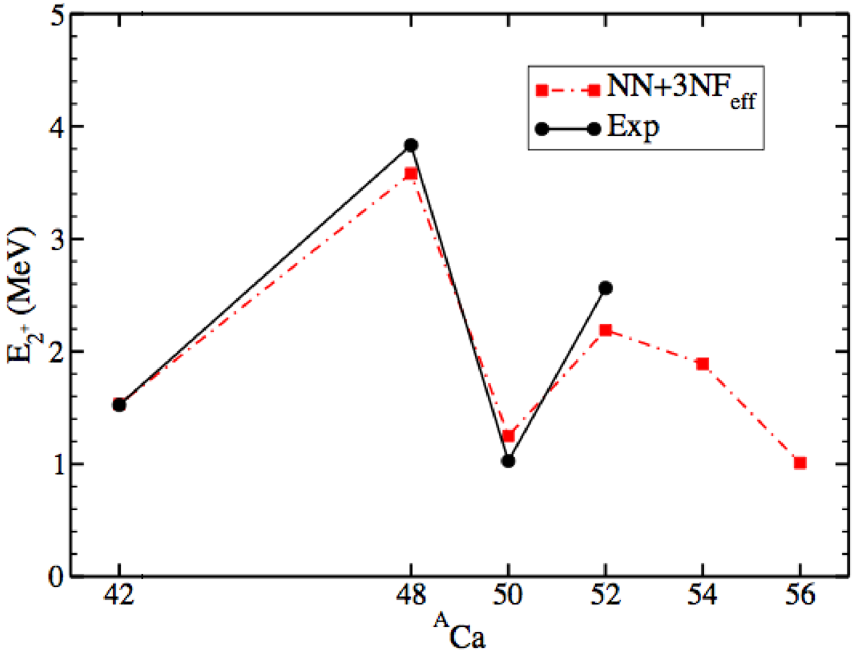

Hagen et al. (2012)

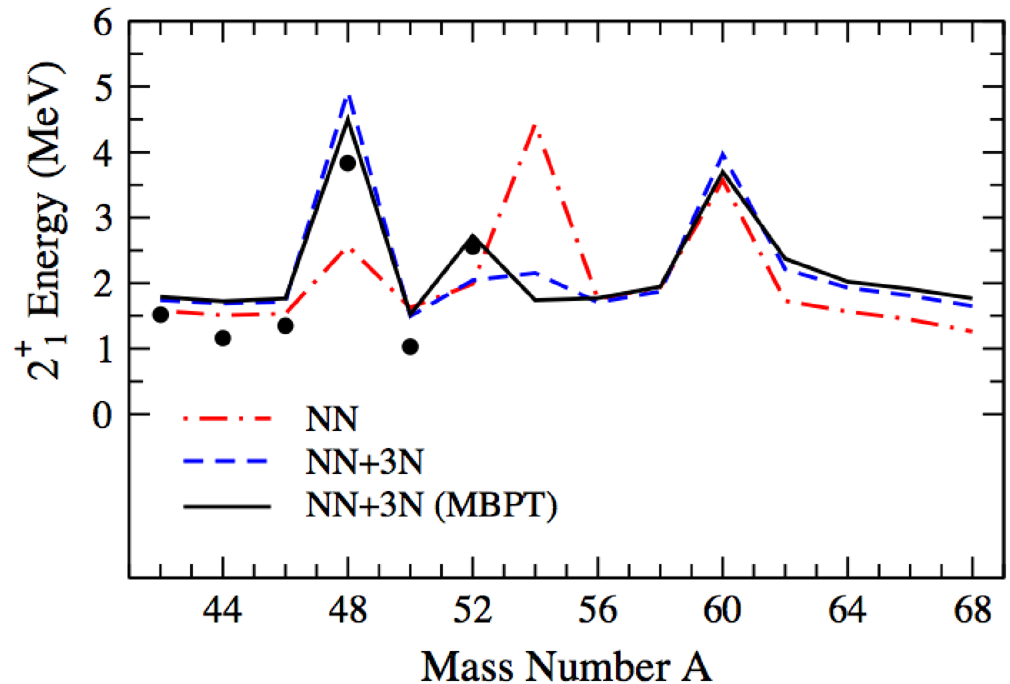

Holt et al. (2012, 2013)

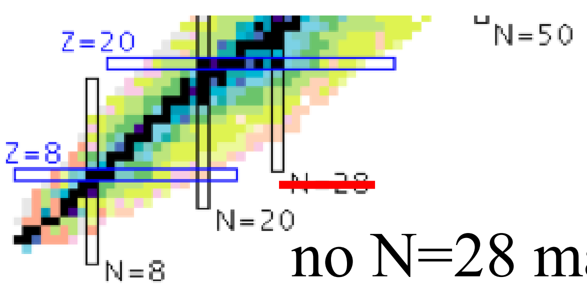

no N=28 magic number from microscopic NN forces

Zuker, Poves,…

Three-body forces and magic numbers

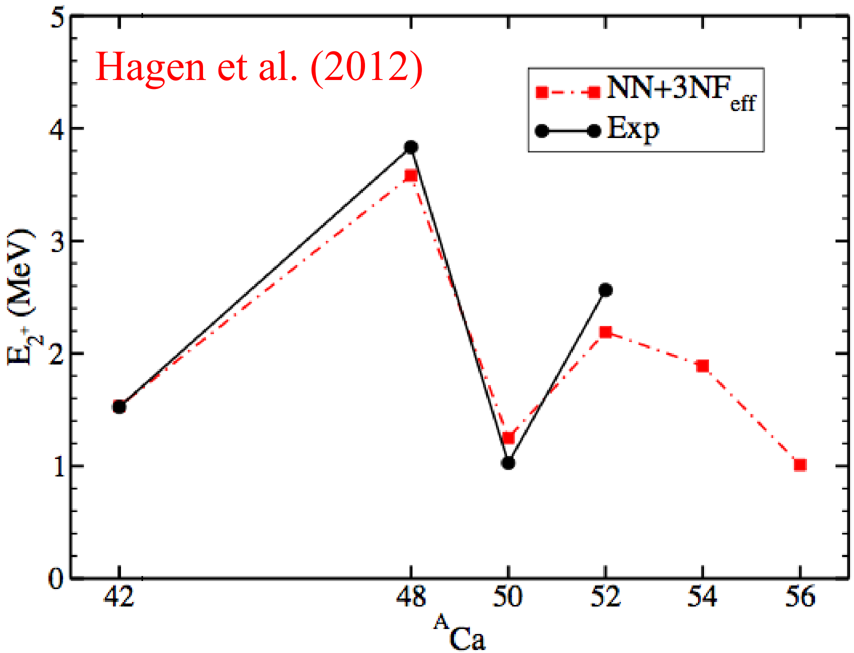

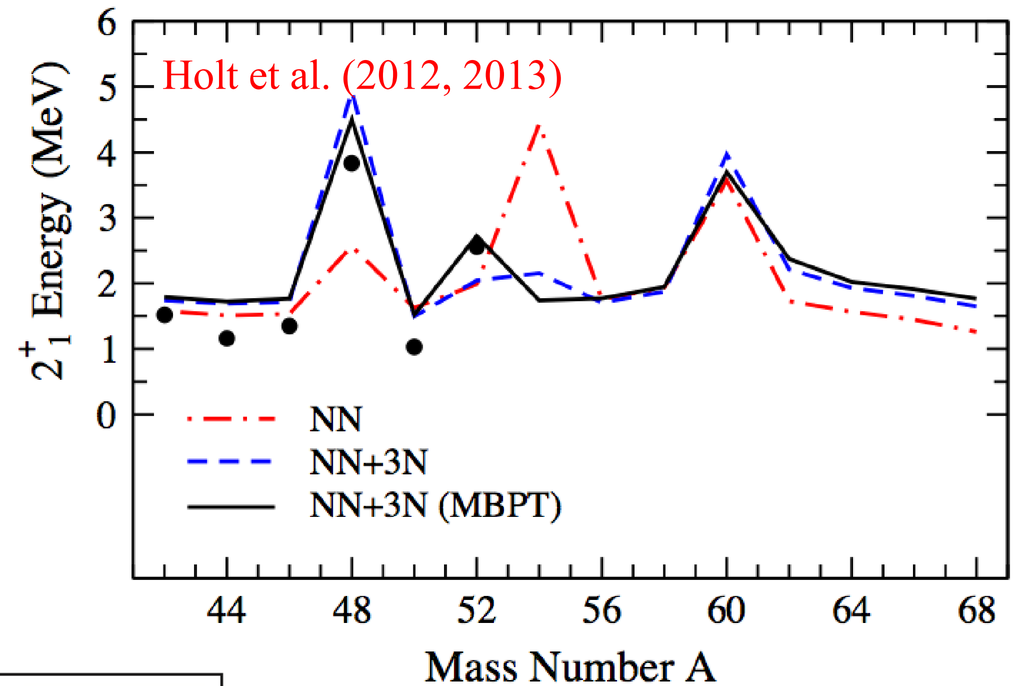

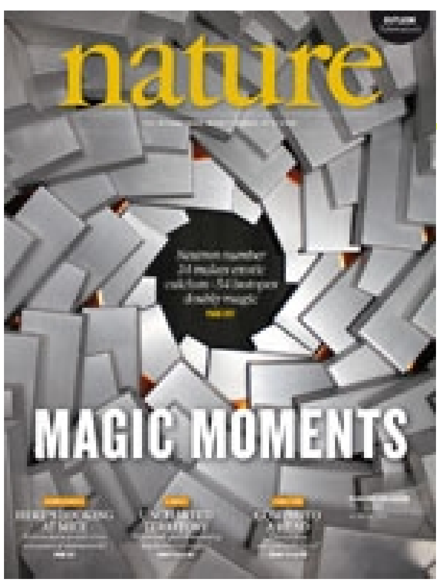

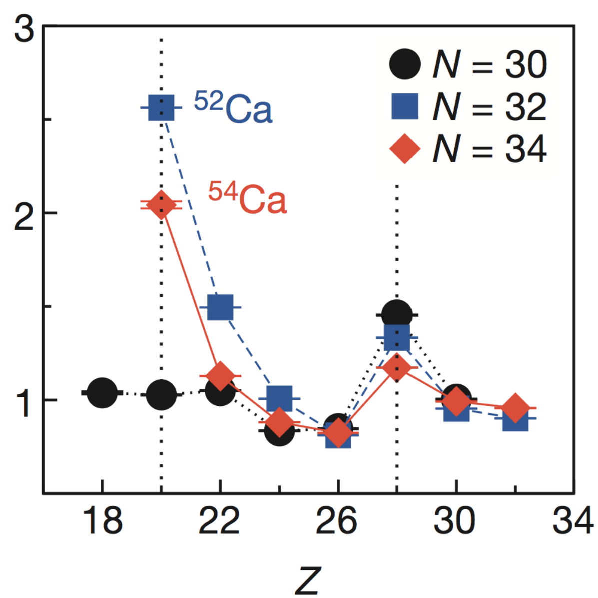

2+ energy measured at RIBF suggests magic number N=34

Steppenbeck et al. (2013)

Evolution to neutron-rich calcium isotopes

repulsive 3N contributions also key for calcium ground-state energies

Holt, Otsuka, AS, Suzuki (2012)

mass measured to 52Ca
shown to exist to 58Ca

gs energy flat with N,
continuum important
for dripline location!

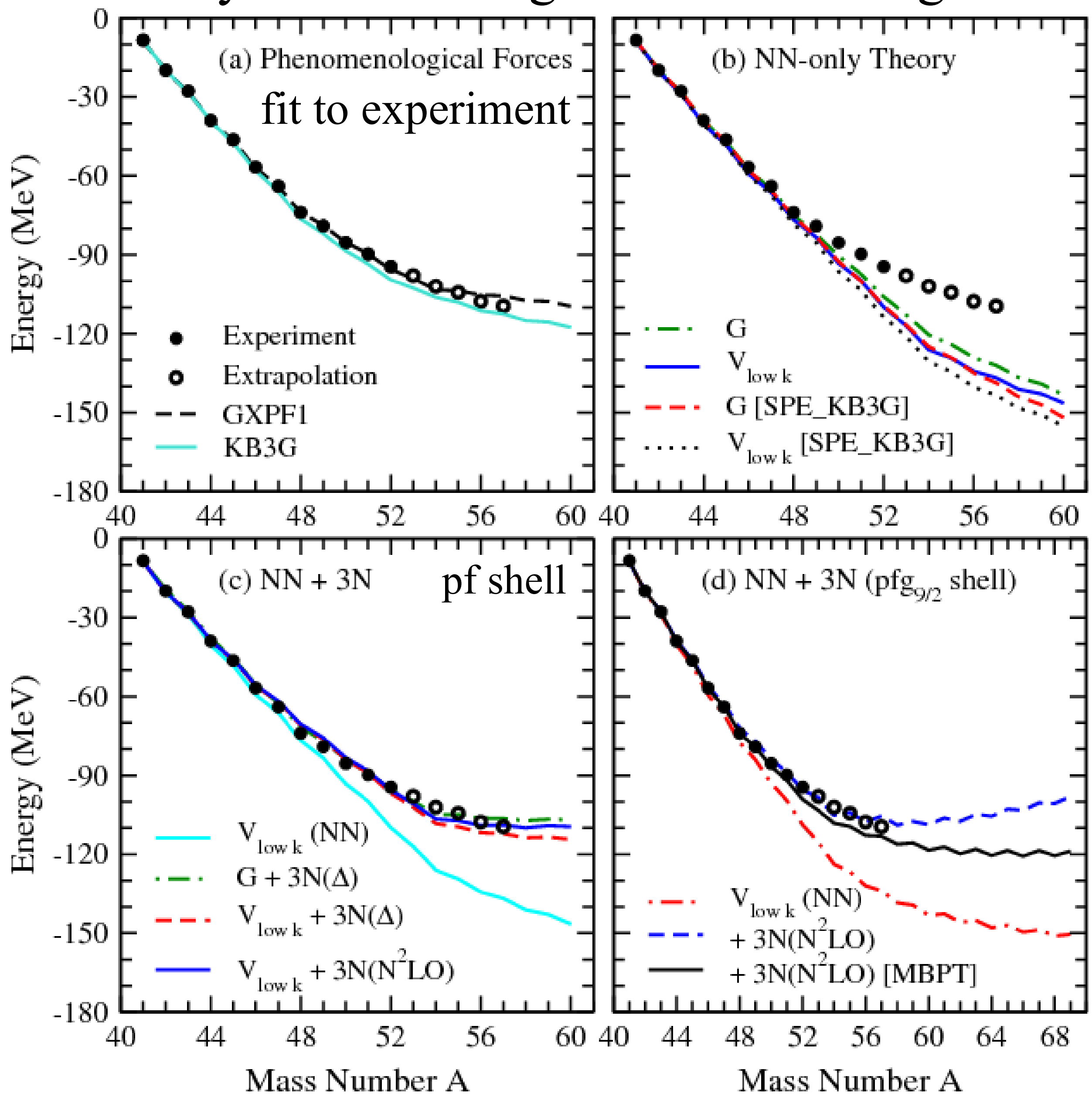

Evolution to neutron-rich calcium isotopes

repulsive 3N contributions also key for calcium ground-state energies

Holt, Otsuka, AS, Suzuki (2012)

mass measured to 52Ca
shown to exist to 58Ca

gs energy flat with N,
continuum important
for dripline location!

see Forssen et al. (2013)

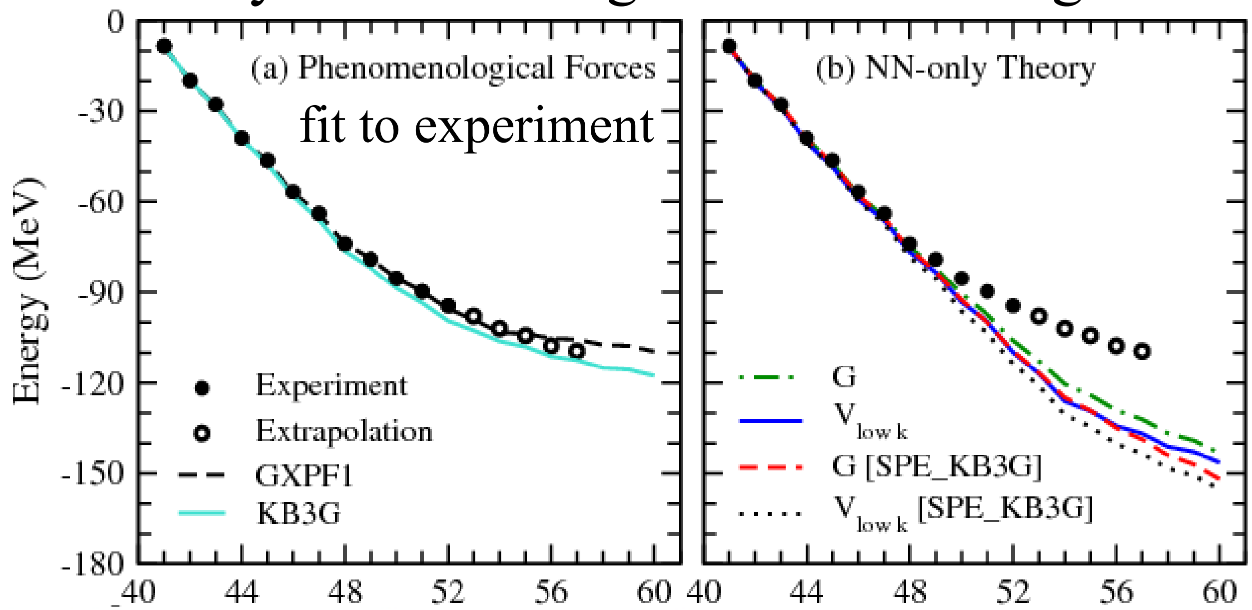

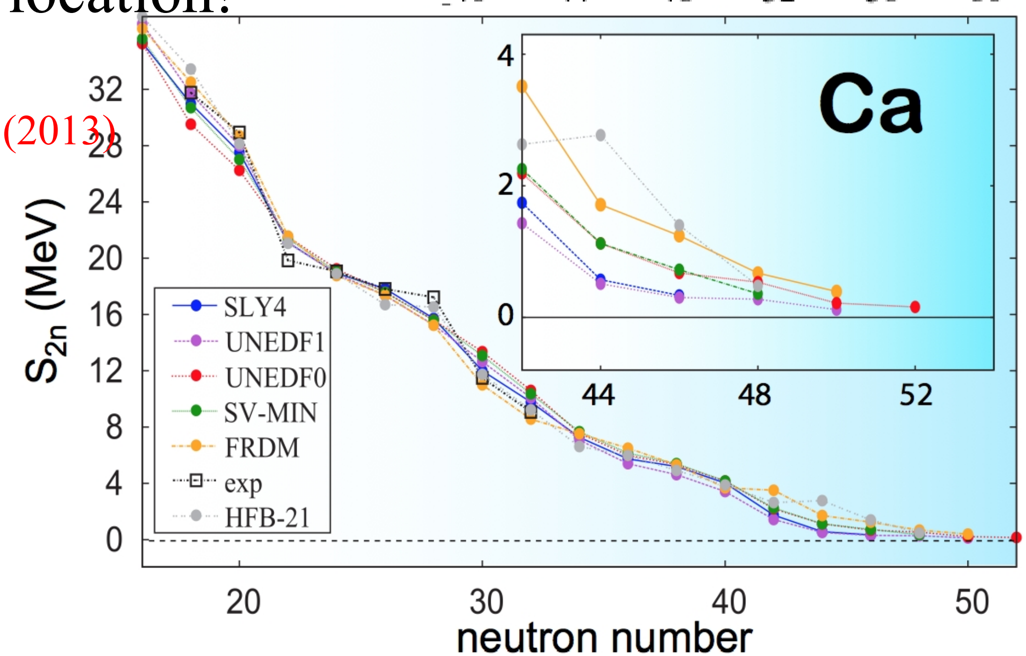

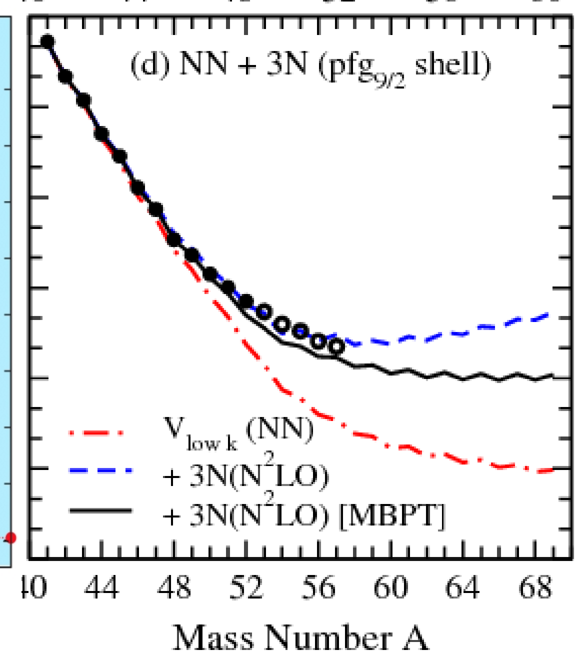

new 51,52Ca TITAN measurements

52Ca is 1.75 MeV more bound compared to atomic mass evaluation

Gallant et al. (2012)

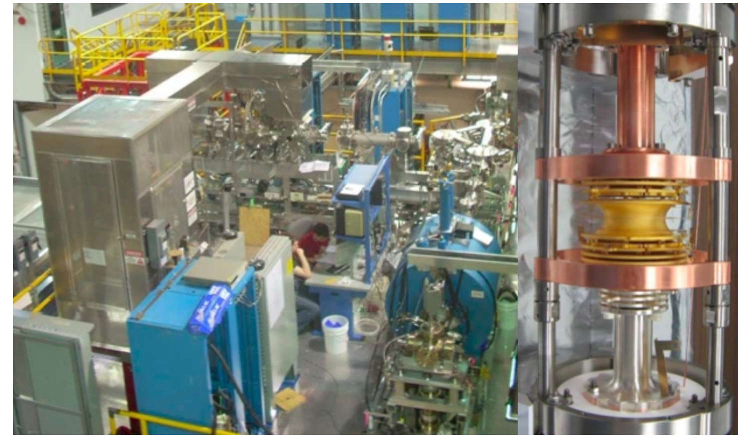

behavior of 2n separation energy S2n agrees with NN+3N predictions

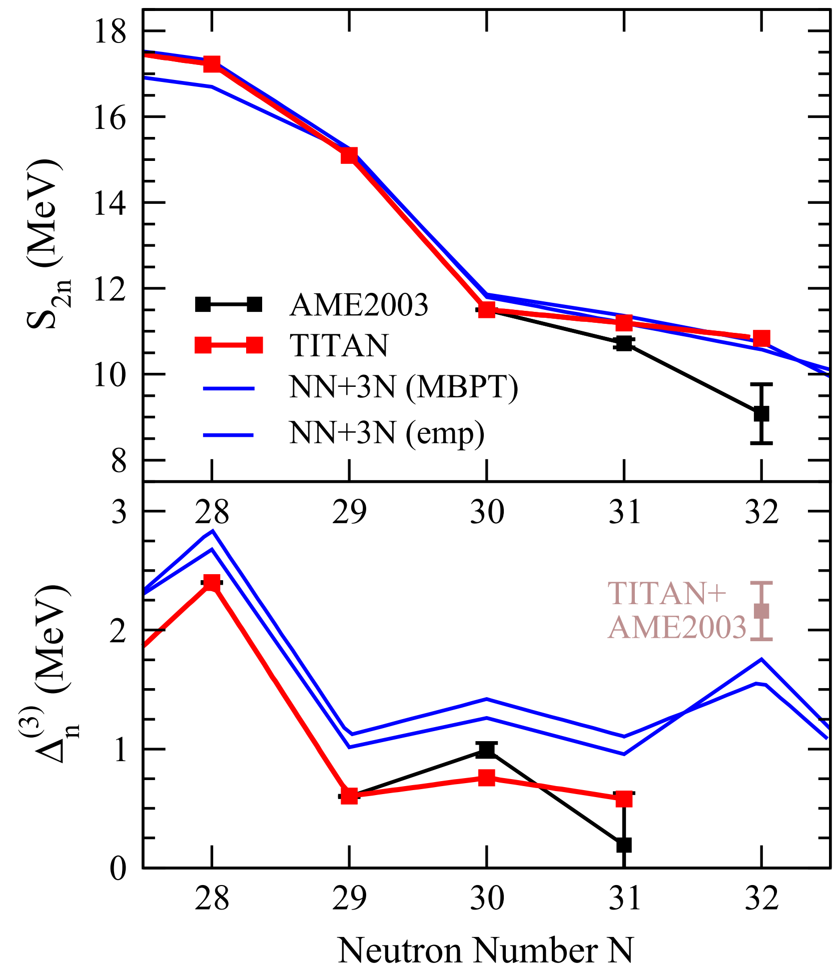

doi:10.1038/nature12226

Masses of exotic calcium isotopes pin down nuclear forces

F. Wienholtz[1], D. Beck[2], K. Blaum[3], Ch. Borgmann[3], M. Breitenfeldt[4], R. B. Cakirli[3,5], S. George[1], F. Herfurth[2], J. D. Holt[6,7], M. Kowalska[8], S. Kreim[3,8], D. Lunney[9], V. Manea[9], J. Menéndez[6,7], D. Neidherr[2], M. Rosenbusch[1], L. Schweikhard[1], A. Schwenk[7,6], J. Simonis[6,7], J. Stanja[10], R. N. Wolf[1] & K. Zuber[10]

53,54Ca masses measured at ISOLTRAP using new MR-TOF mass spectrometer

establish prominent N=32 shell closure in calcium

excellent agreement with theoretical predictions

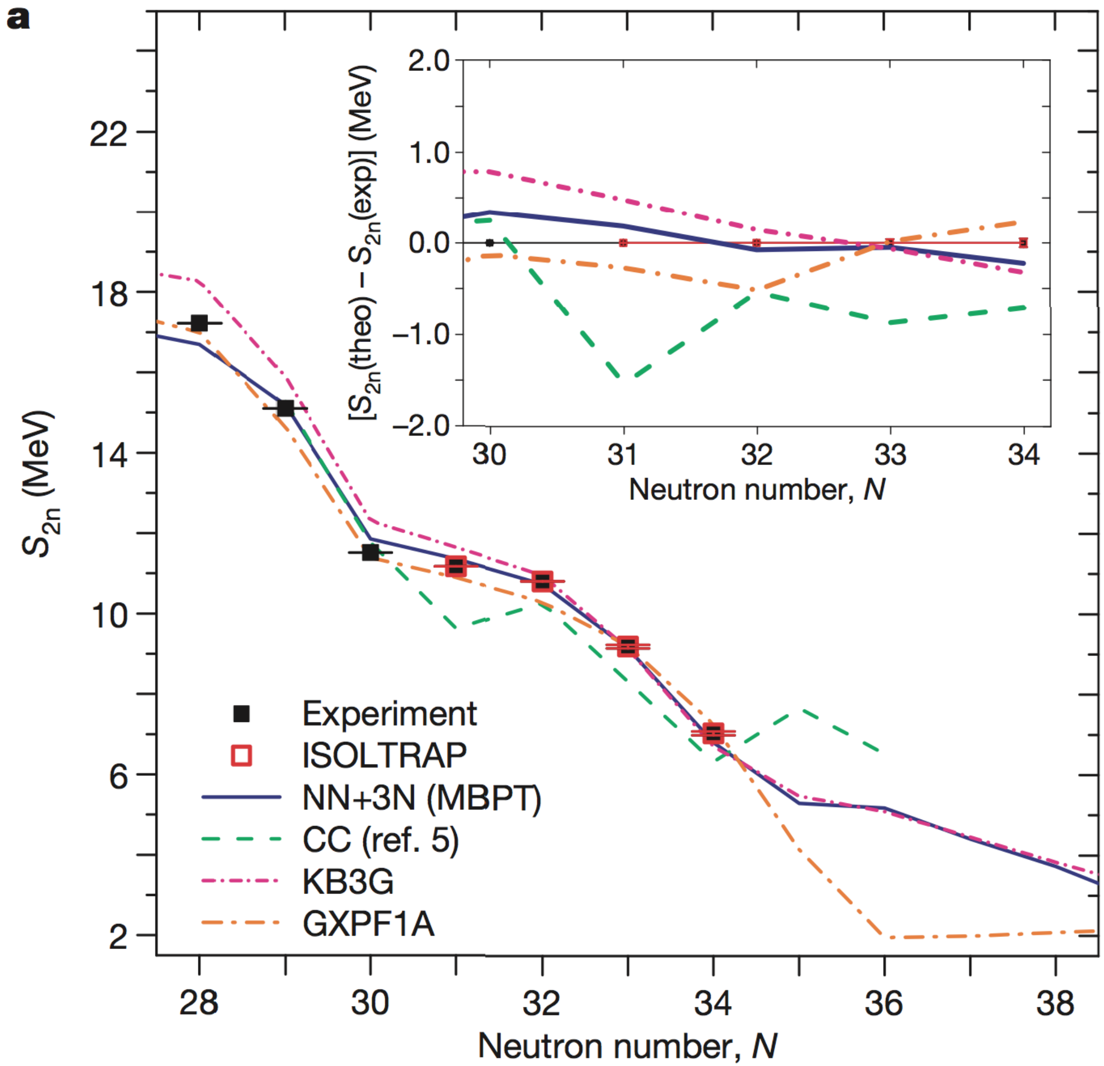

doi:10.1038/nature12226

Masses of exotic calcium isotopes pin down nuclear forces

F. Wienholtz[1], D. Beck[2], K. Blaum[3], Ch. Borgmann[3], M. Breitenfeldt[4], R. B. Cakirli[3,5], S. George[1], F. Herfurth[2], J. D. Holt[6,7], M. Kowalska[8], S. Kreim[3,8], D. Lunney[9], V. Manea[9], J. Menéndez[6,7], D. Neidherr[2], M. Rosenbusch[1], L. Schweikhard[1], A. Schwenk[7,6], J. Simonis[6,7], J. Stanja[10], R. N. Wolf[1] & K. Zuber[10]

overall good agreement with density functional predictions

challenge to reproduce shell closures

cf. N=50, 82, 126 "arches"
Bender et al. (2005)

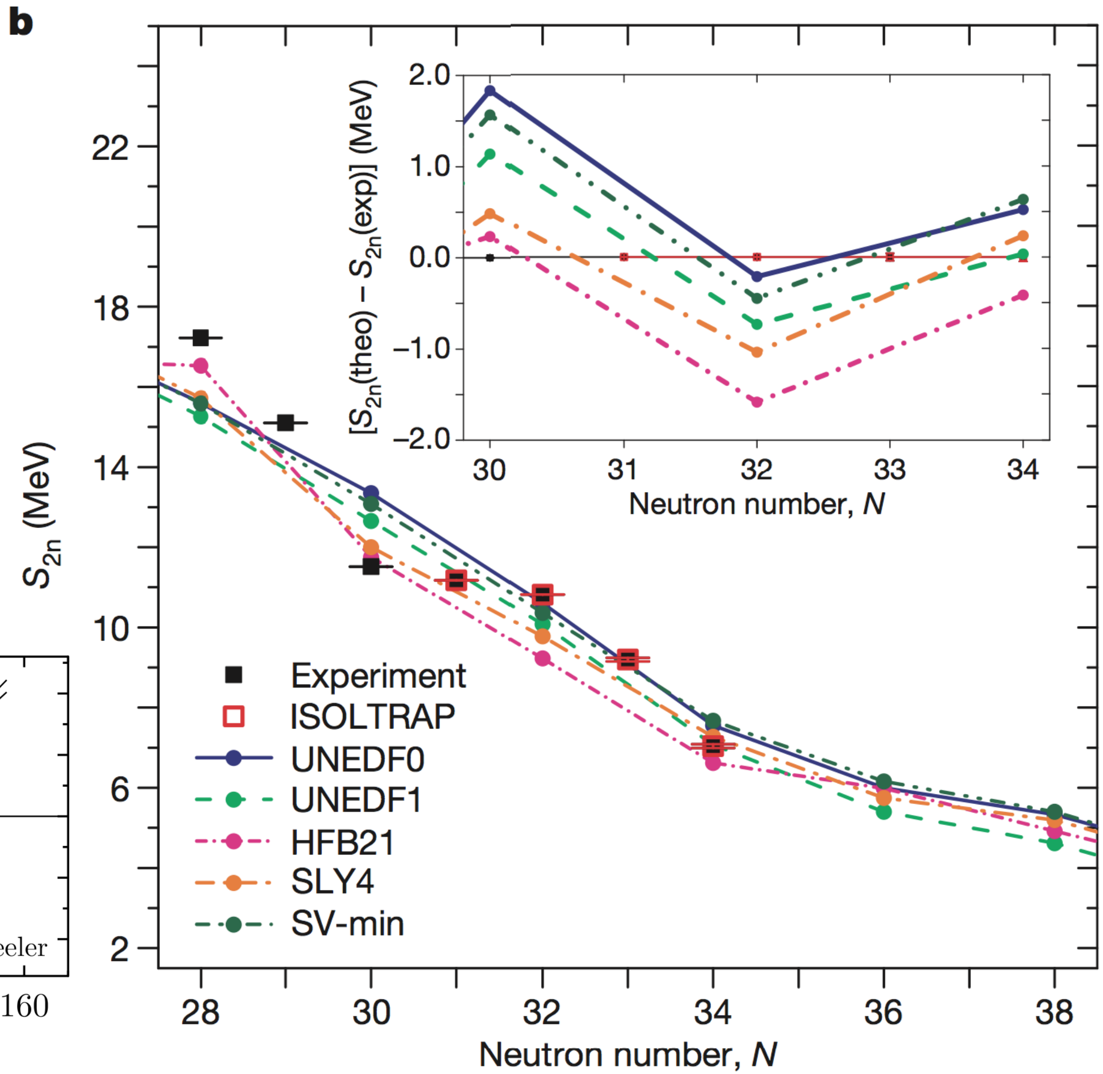

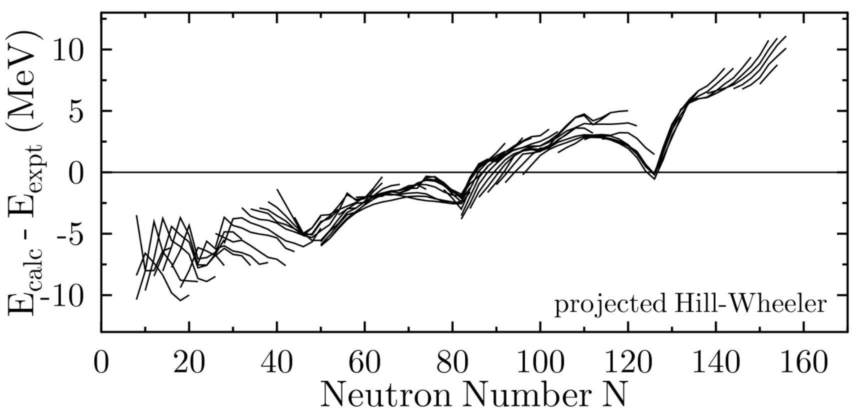

3N forces and proton-rich nuclei Holt, Menendez, AS (2013)

first results with 3N forces for ground and excited states of N=8, 20

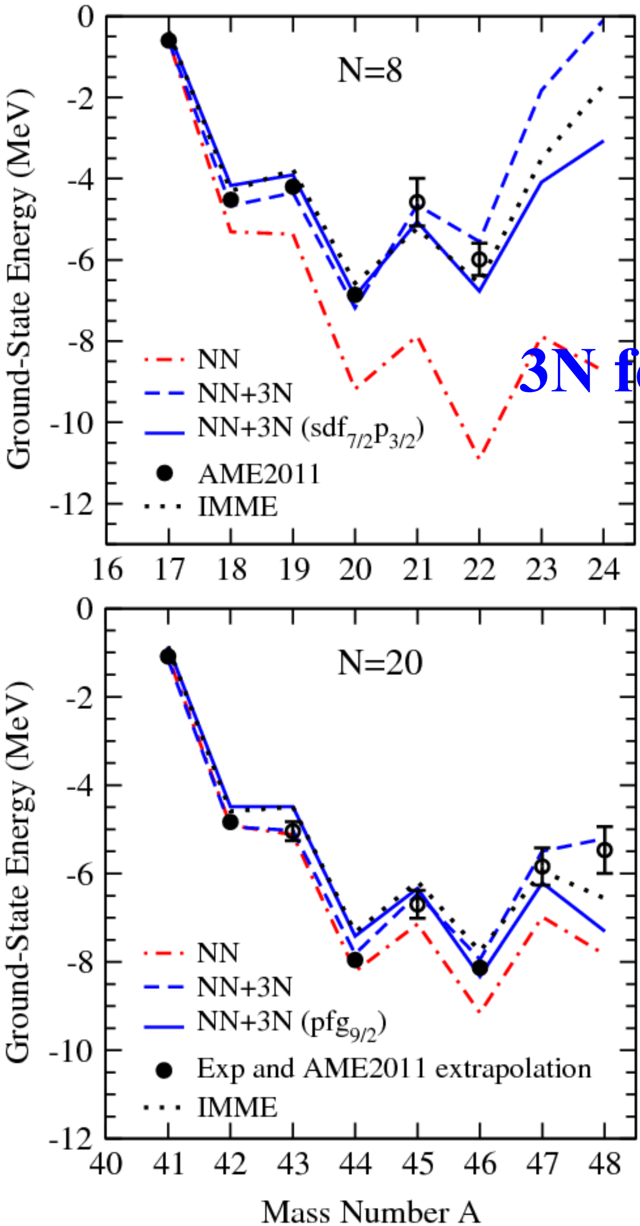

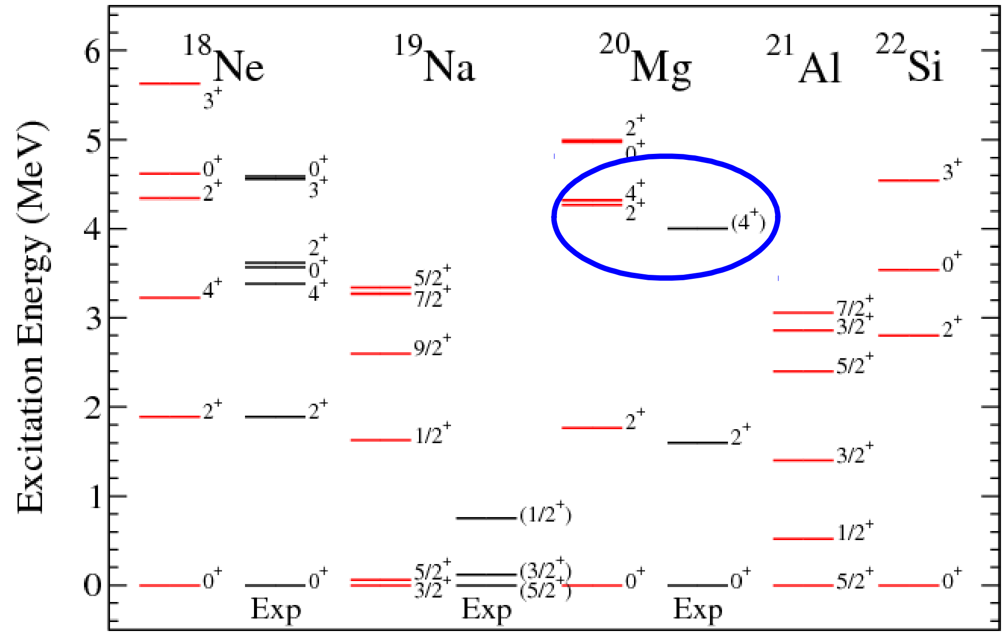

prediction for 20Mg agrees with new state observed at GSI Mukha, private comm.

Neutron matter and neutron stars

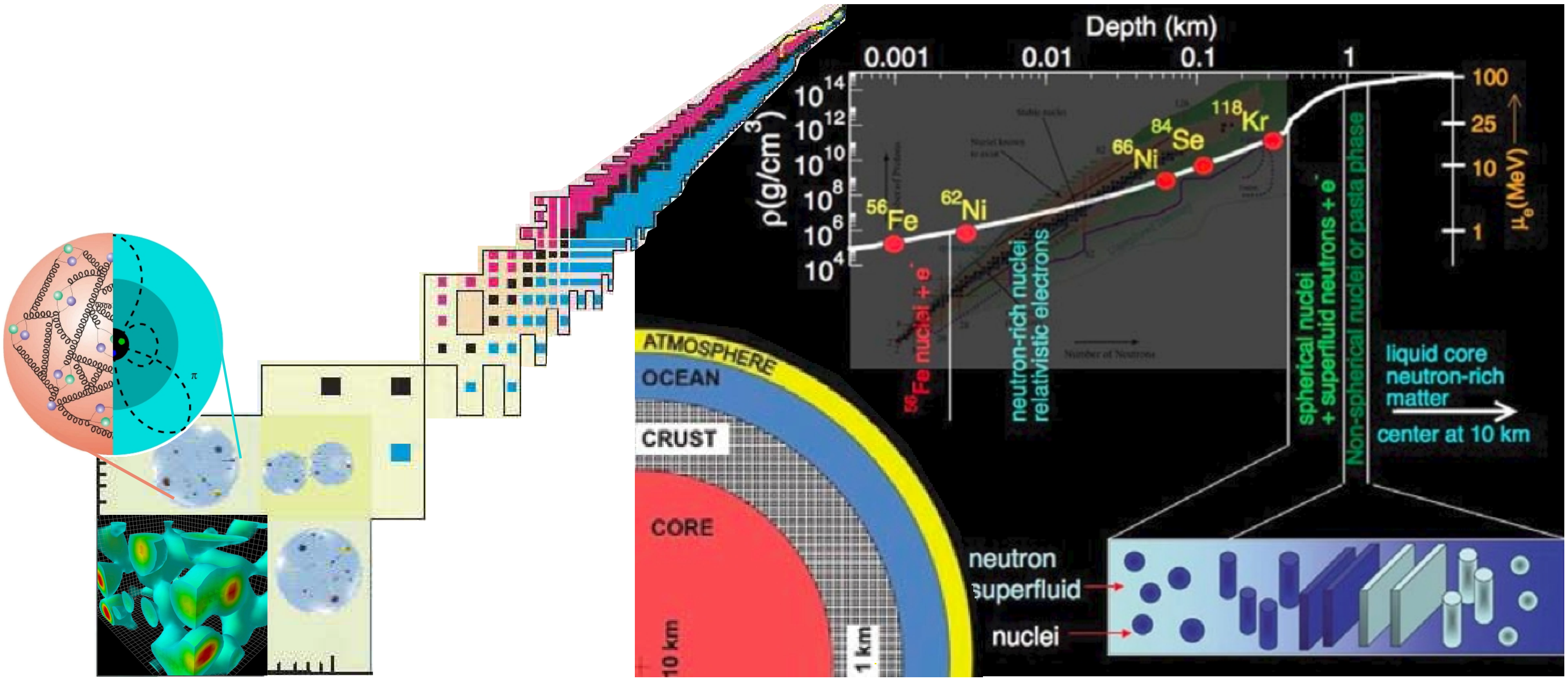

Chiral effective field theory for nuclear forces

Separation of scales: low momenta $\frac{1}{\lambda} = Q \ll \Lambda_b$ breakdown scale ~500 MeV

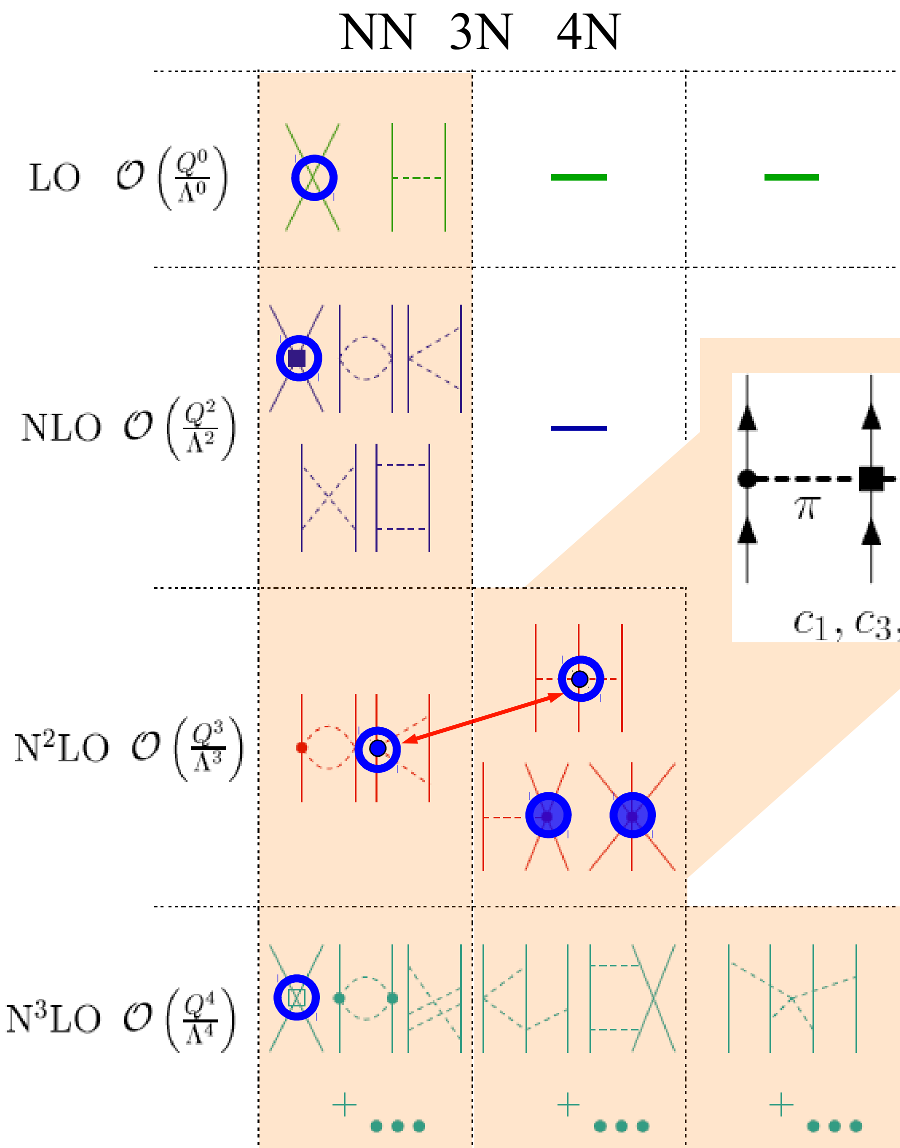

cD, cE don't contribute for neutrons because of Pauli principle and pion coupling to spin, also for c4

Hebeler, AS (2010)

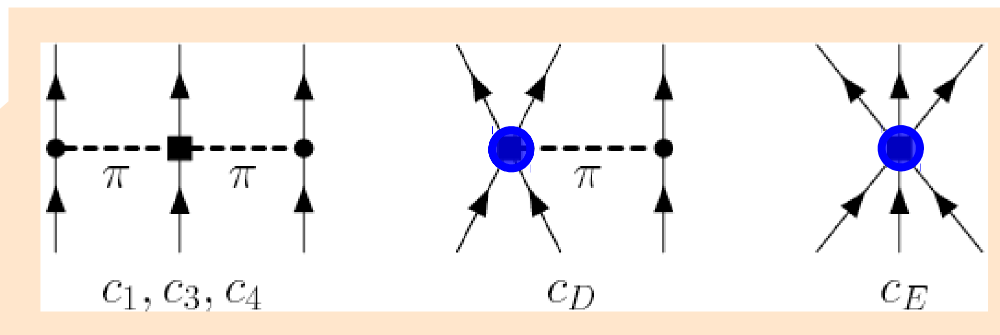

all 3- and 4-neutron forces are predicted to N3LO!

study 3N and 4N in neutron matter

Tews, Krüger, Hebeler, AS (2013)

Weinberg, van Kolck, Kaplan, Savage, Wise, Bernard, Epelbaum, Kaiser, Machleidt, Meissner,…

Complete N3LO calculation of neutron matter

first complete N3LO result Tews, Krüger, Hebeler, AS (2013)

includes uncertainties from NN, 3N (dominates), 4N

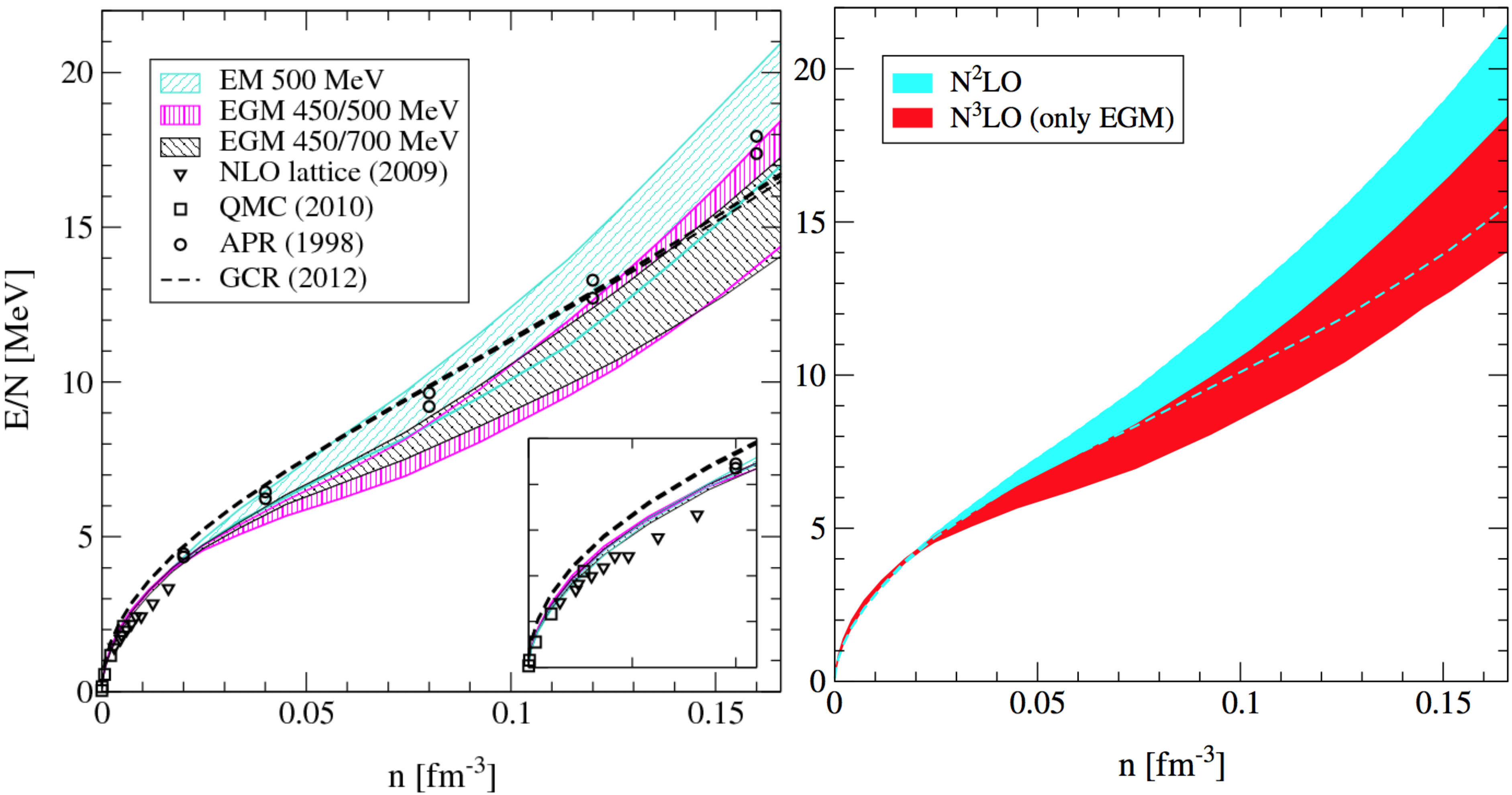

Neutron skin of 208Pb

probes neutron matter energy/pressure,
neutron matter band predicts
neutron skin of 208Pb: 0.17±0.03 fm (±18% !)
Hebeler et al. (2010)

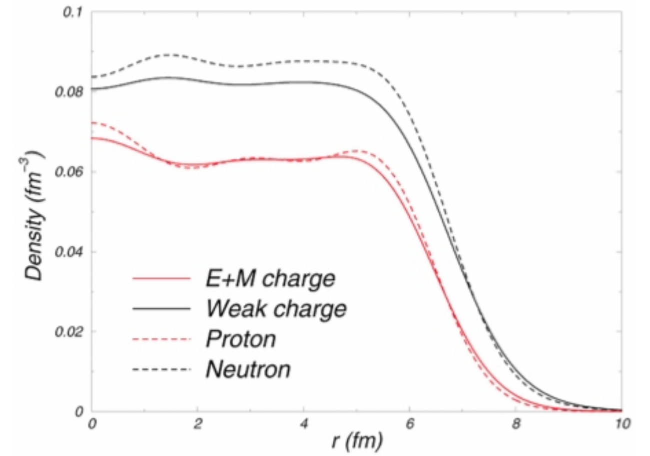

Neutron skin of 208Pb

probes neutron matter energy/pressure,
neutron matter band predicts
neutron skin of 208Pb: 0.17±0.03 fm (±18% !)
Hebeler et al. (2010)

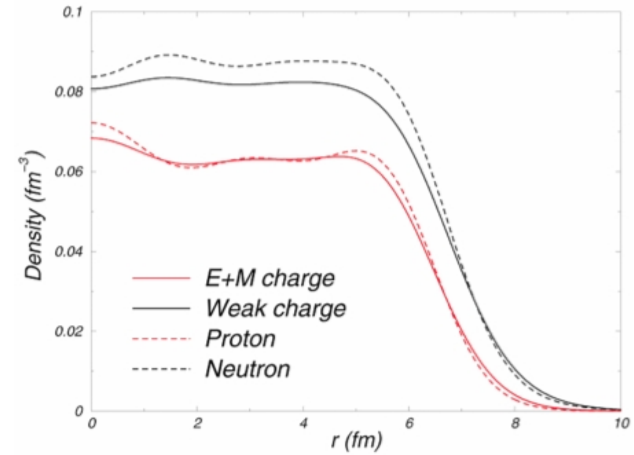

in excellent agreement with extraction from complete E1 response
0.156+0.025-0.021 fm

PRL 107, 062502 (2011) PHYSICAL REVIEW LETTERS week ending 5 AUGUST 2011

Complete Electric Dipole Response and the Neutron Skin in ^{208}Pb

A benchmark experiment on ^{208}Pb shows that polarized proton inelastic scattering at very forward angles including 0° is a powerful tool for high-resolution studies of electric dipole ($E1$) and spin magnetic dipole ($M1$) modes in nuclei over a broad excitation energy range to test up-to-date nuclear models. The extracted $E1$ polarizability leads to a neutron skin thickness $r_{\rm skin} = 0.156^{+0.025}_{-0.021}$ fm in ^{208}Pb derived within

PREX: neutron skin from parity-violating electron-scattering at JLAB
electron exchanges Z-b
goal II: ±0.06 fm

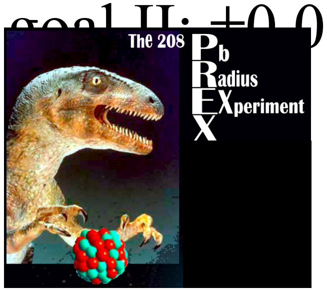

PRL 108, 112502 (2012) PHYSICAL REVIEW LETTERS week ending 16 MARCH 2012

Measurement of the Neutron Radius of ^{208}Pb through Parity Violation in Electron Scattering

We report the first measurement of the parity-violating asymmetry $A_{\rm PV}$ in the elastic scattering of polarized electrons from ^{208}Pb. $A_{\rm PV}$ is sensitive to the radius of the neutron distribution (R_n). The result $A_{\rm PV} = 0.656 \pm 0.060({\rm stat}) \pm 0.014({\rm syst})$ ppm corresponds to a difference between the radii of the neutron and proton distributions $R_n - R_p = 0.33^{+0.16}_{-0.18}$ fm and provides the first electroweak observation of the neutron skin which is expected in a heavy, neutron-rich nucleus.

Symmetry energy and pressure of neutron matter

neutron matter band predicts symmetry energy Sv and its density derivative L

comparison to experimental and observational constraints
Lattimer, Lim (2013)

neutron matter constraints
H: Hebeler et al. (2010, 2013)

G: Gandolfi et al. (2011)

microscopic calculations provide tight constraints!

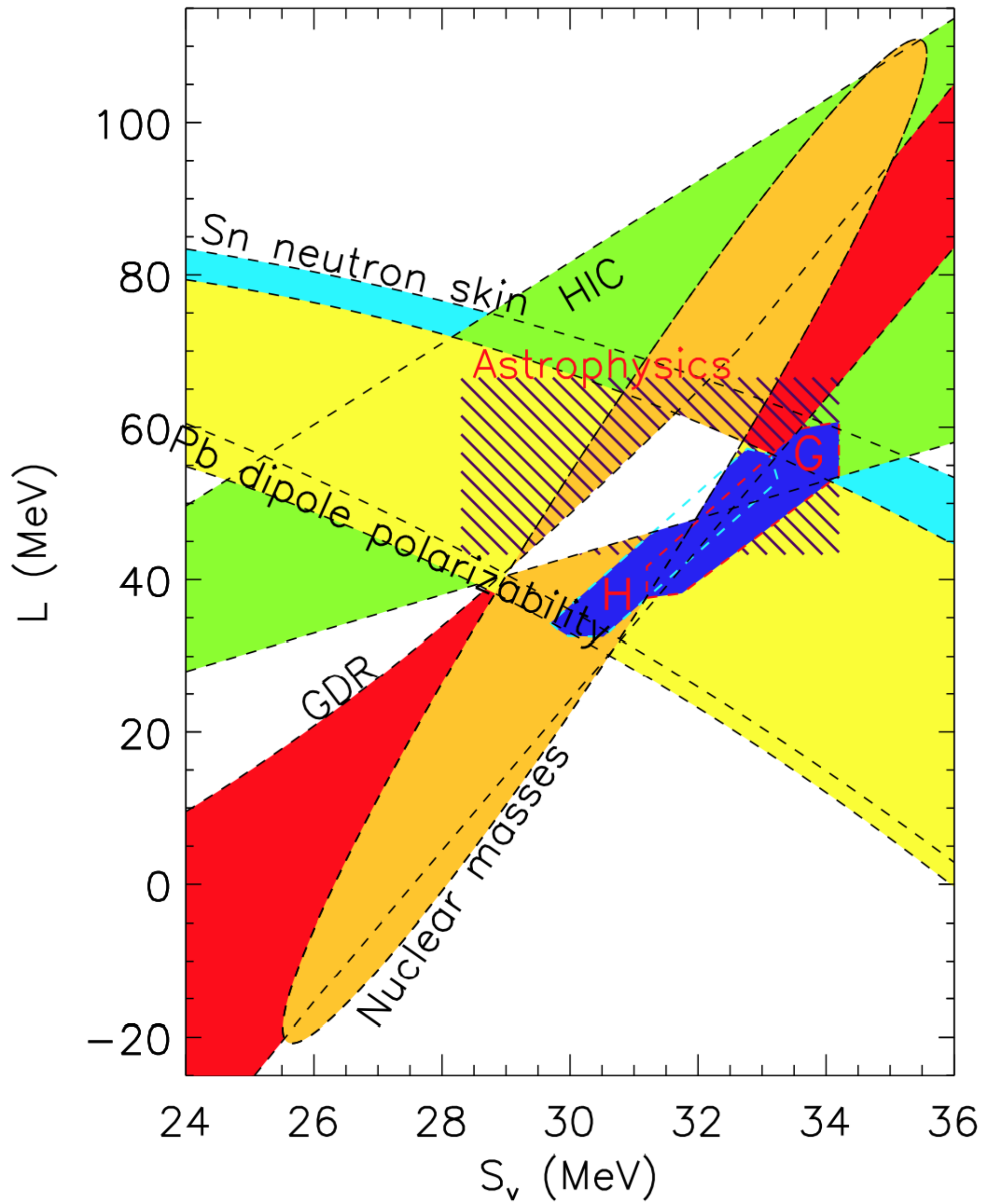

Ab-initio calculations of asymmetric matter Drischler, Soma, AS (2013)

Esym comparison with extraction from isobaric analogue states (IAS)

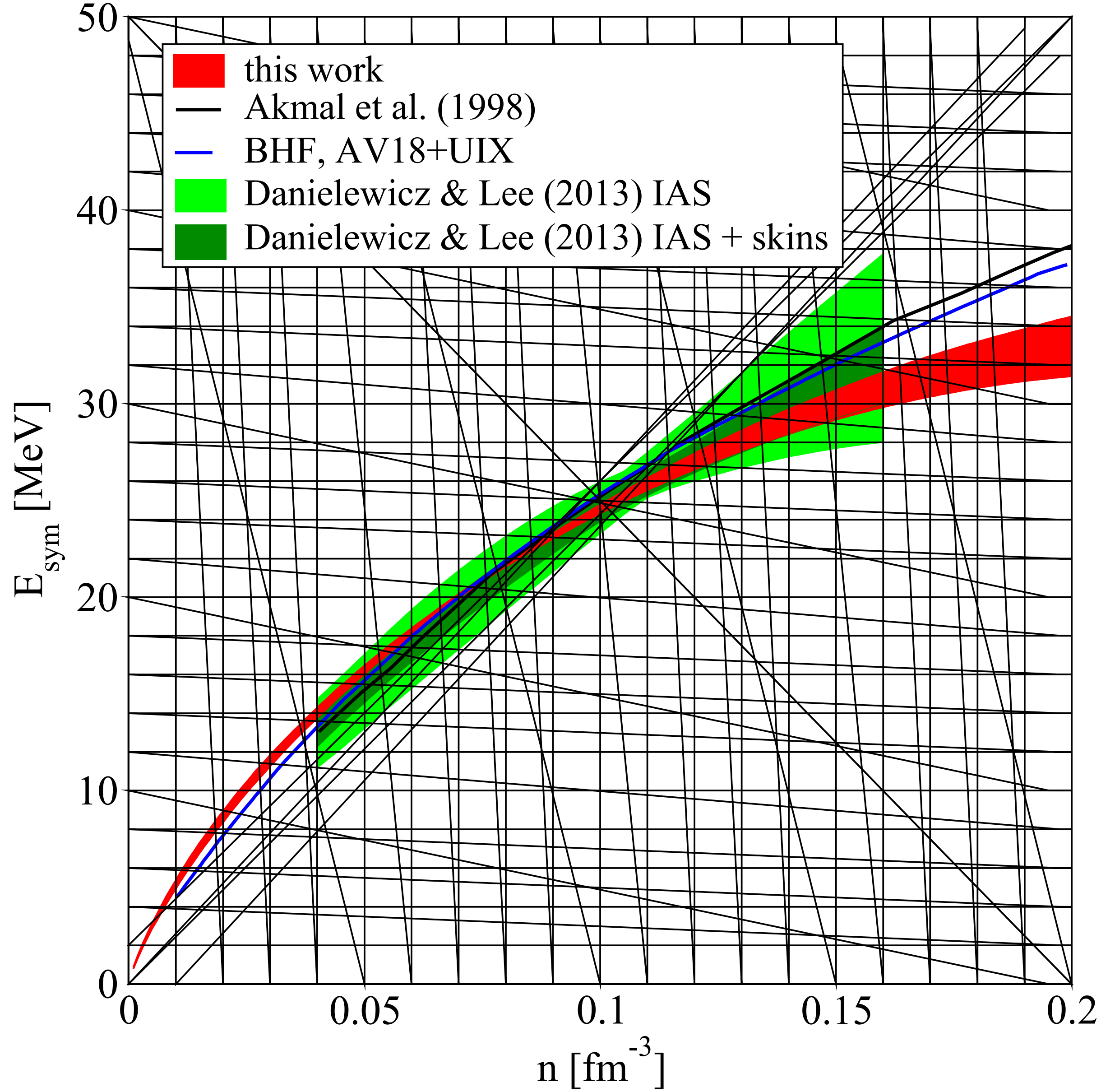

Complete N3LO calculation of neutron matter

first complete N3LO result Tews, Krüger, Hebeler, AS (2013)

includes uncertainties from NN, 3N (dominates), 4N

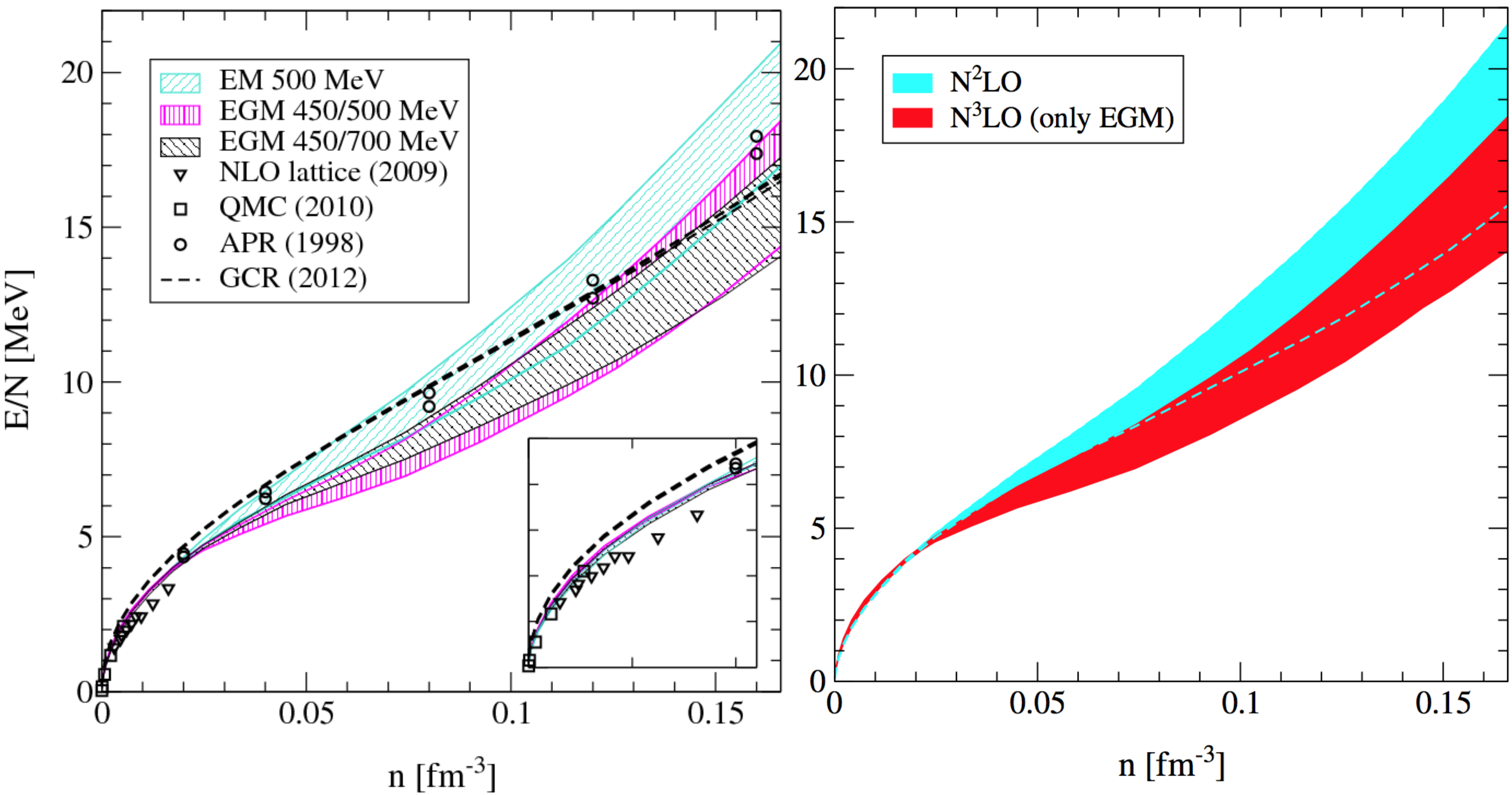

Discovery of the heaviest neutron star

A two-solar-mass neutron star measured using Shapiro delay

P. B. Demorest[1], T. Pennucci[2], S. M. Ransom[1], M. S. E. Roberts[3] & J. W. T. Hessels[4,5]

Nature (2010)

direct measurement of neutron star mass from increase in signal travel time near companion

J1614-2230
most edge-on binary pulsar known (89.17°)
+ massive white dwarf companion (0.5 Msun)

heaviest neutron star with 1.97±0.04 Msun

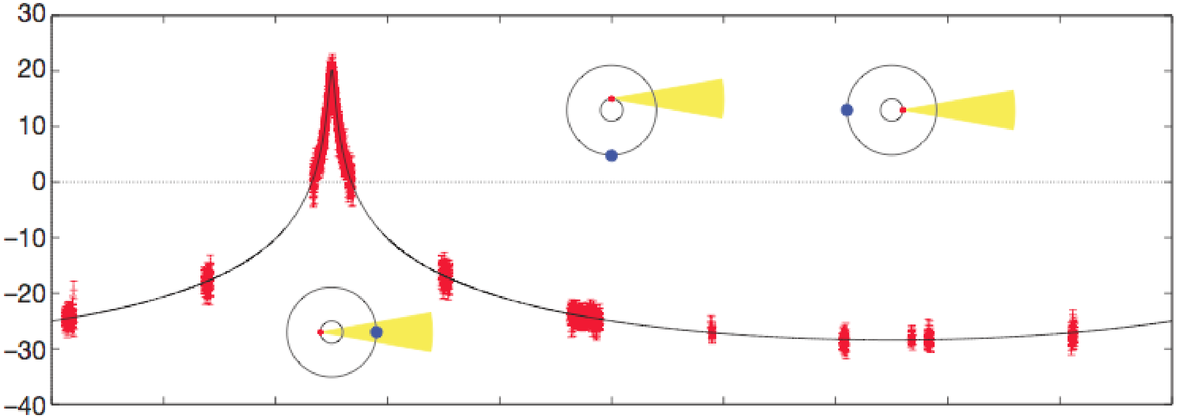

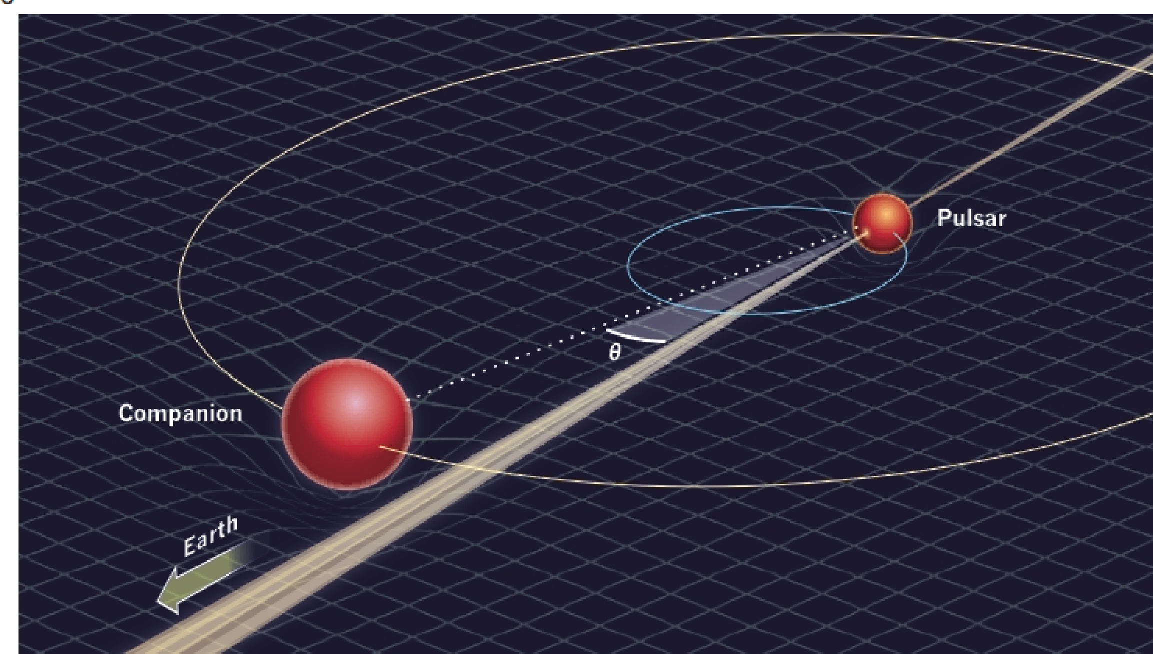

Discovery of the heaviest neutron star (2013)

RESEARCH ARTICLE SUMMARY

A Massive Pulsar in a Compact Relativistic Binary

John Antoniadis,* Paulo C. C. Freire, Norbert Wex, Thomas M. Tauris, Ryan S. Lynch, Marten H. van Kerkwijk, Michael Kramer, Cees Bassa, Vik S. Dhillon, Thomas Driebe, Jason W. T. Hessels, Victoria M. Kaspi, Vladislav I. Kondratiev, Norbert Langer, Thomas R. Marsh, Maura A. McLaughlin, Timothy T. Pennucci, Scott M. Ransom, Ingrid H. Stairs, Joeri van Leeuwen, Joris P. W. Verbiest, David G. Whelan

Introduction: Neutron stars with masses above 1.8 solar masses ($M_\odot$), possess extreme gravitational fields, which may give rise to phenomena outside general relativity. Hitherto, these strong-field deviations have not been probed by experiment, because they become observable only in tight binaries containing a high-mass pulsar and where orbital decay resulting from emission of gravitational waves can be tested. Understanding the origin of such a system would also help to answer fundamental questions of close-binary evolution.

Methods: We report on radio-timing observations of the pulsar J0348+0432 and phase-resolved optical spectroscopy of its white-dwarf companion, which is in a 2.46-hour orbit. We used these to derive the component masses and orbital parameters, infer the system's motion, and constrain its age.

Results: We find that the white dwarf has a mass of $0.172 \pm 0.003\ M_\odot$, which, combined with orbital velocity measurements, yields a pulsar mass of $2.01 \pm 0.04\ M_\odot$. Additionally, over a span of 2 years, we observed a significant decrease in the orbital period, $\dot{P}_b^{obs} = -8.6 \pm 1.4\ \mu s\ year^{-1}$ in our radio-timing data.

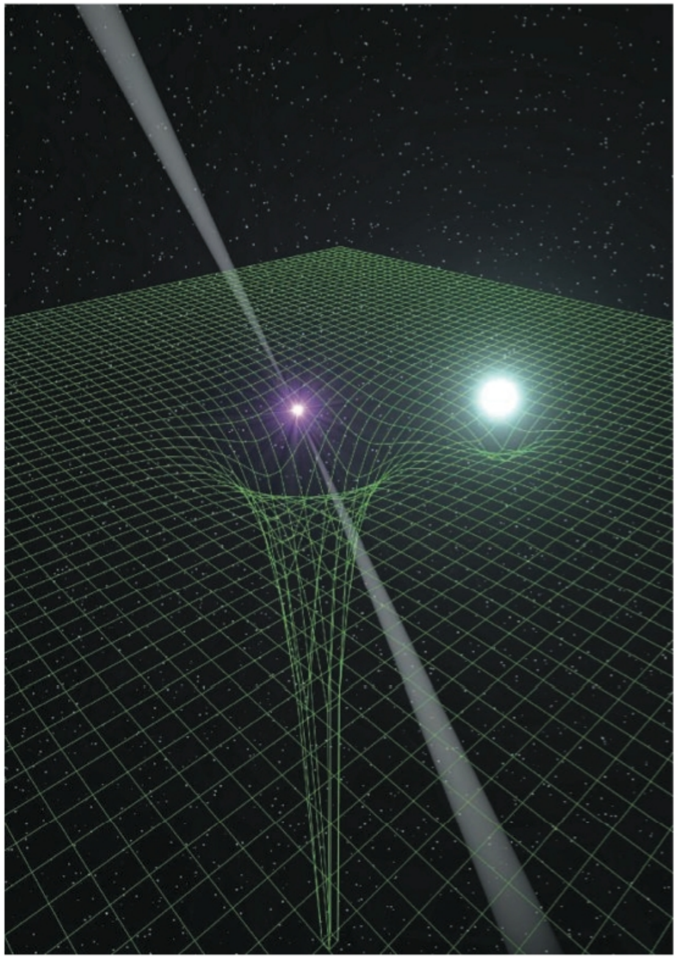

Artist's impression of the PSR J0348+0432 system. The compact pulsar (with beams of radio emission) produces a strong distortion of spacetime (illustrated by the green mesh). Conversely, spacetime around its white dwarf companion (in light blue) is substantially less curved. According to relativistic theories of gravity, the binary system is subject to energy loss by gravitational waves.

Impact on neutron stars Hebeler et al. (2010, 2013)

Equation of state/pressure for neutron-star matter (includes small Ye,p)

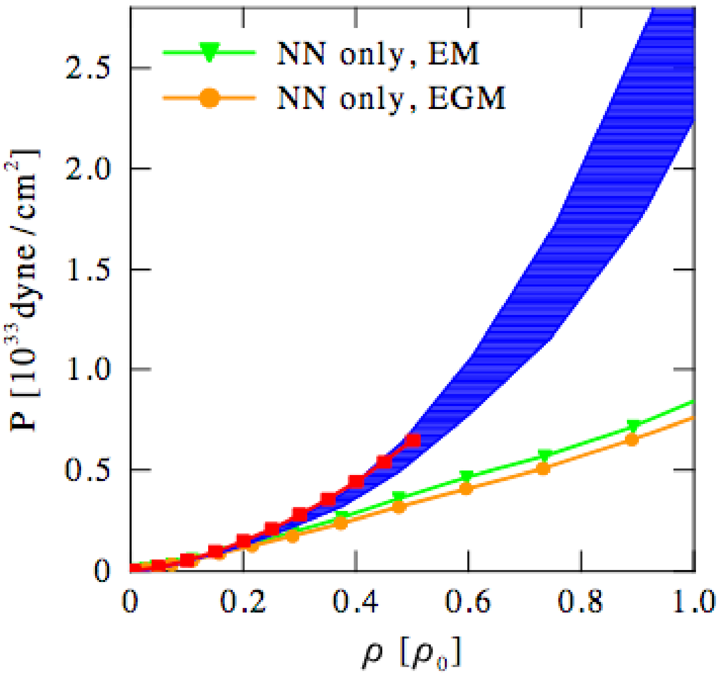

pressure below nuclear densities agrees with standard crust equation of state only after 3N forces are included

Impact on neutron stars Hebeler et al. (2010, 2013)

Equation of state/pressure for neutron-star matter (includes small Ye,p)

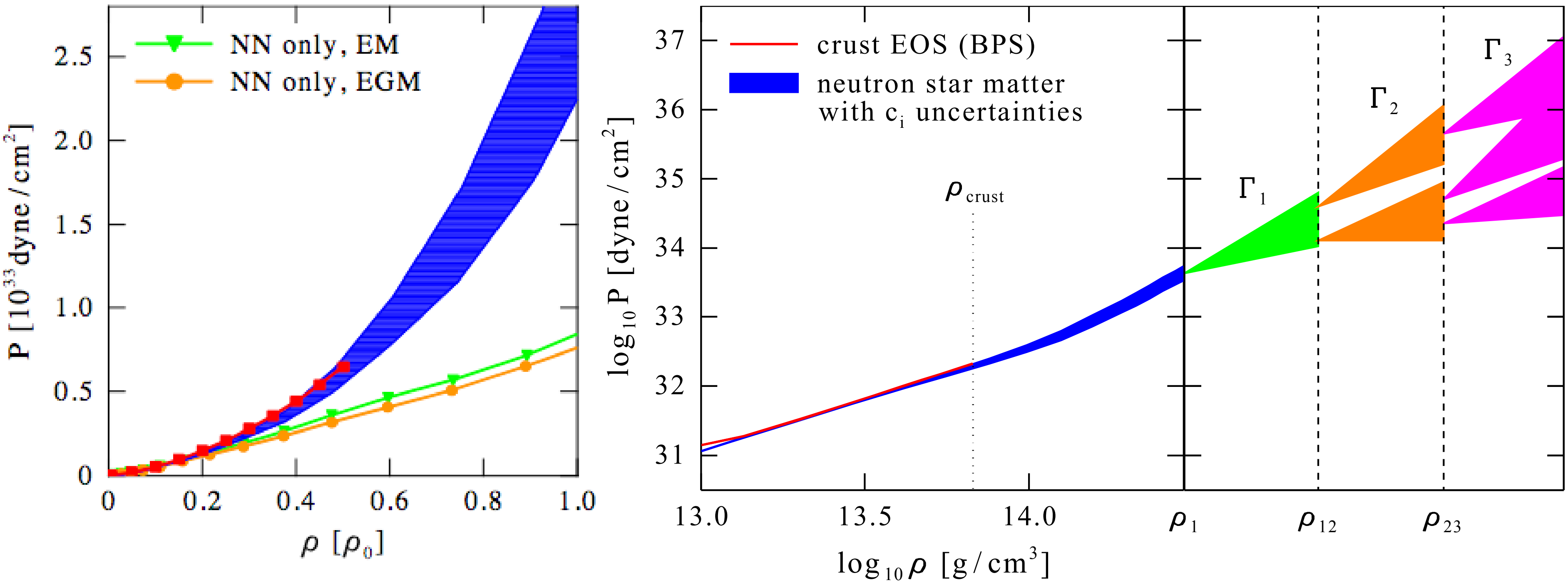

pressure below nuclear densities agrees with standard crust equation of state only after 3N forces are included

extend uncertainty band to higher densities using piecewise polytropes allow for soft regions

Impact on neutron stars Hebeler et al. (2010, 2013)

constrain high-density EOS by causality, require to support 1.97 Msun star

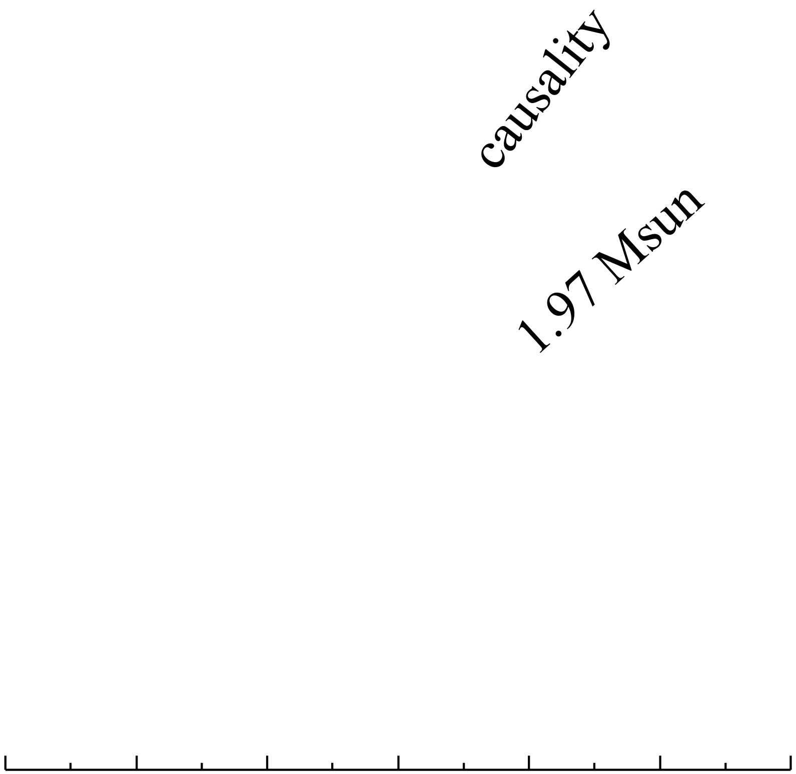

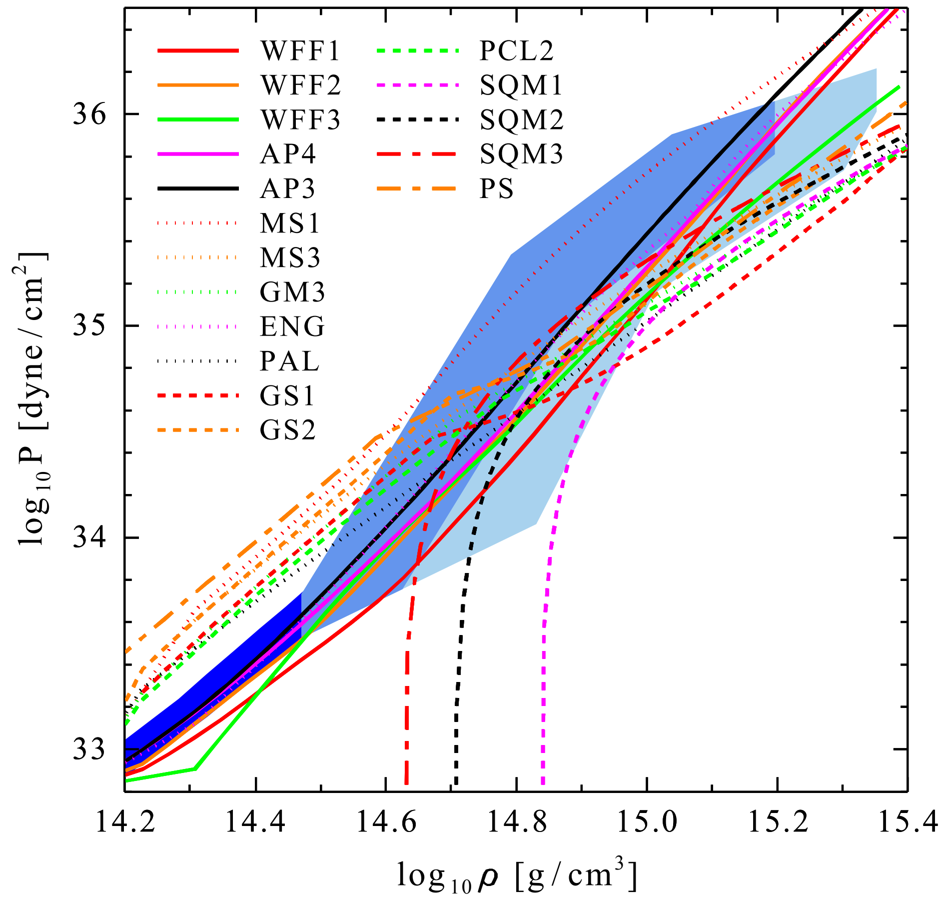

low-density pressure sets scale, chiral EFT interactions provide strong constraints, ruling out many model equations of state

Impact on neutron stars Hebeler et al. (2010, 2013)

constrain high-density EOS by causality, require to support 1.97 Msun star

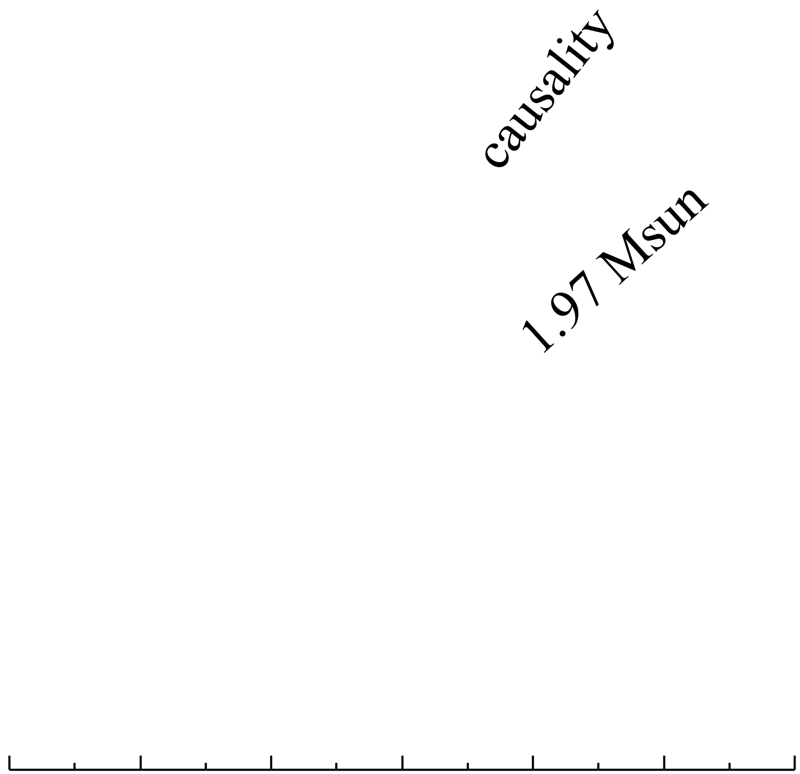

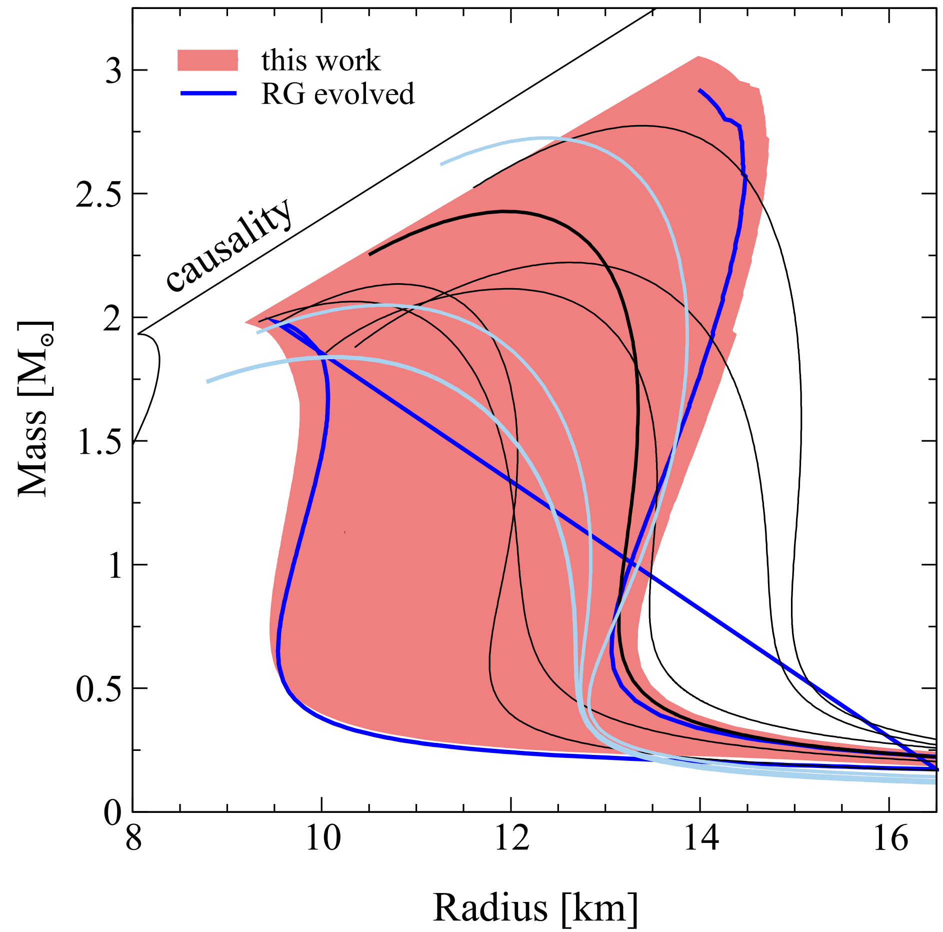

low-density pressure sets scale, chiral EFT interactions provide strong constraints, ruling out many model equations of state

Impact on neutron stars Hebeler et al. (2010, 2013)

constrain high-density EOS by causality, require to support 1.97 Msun

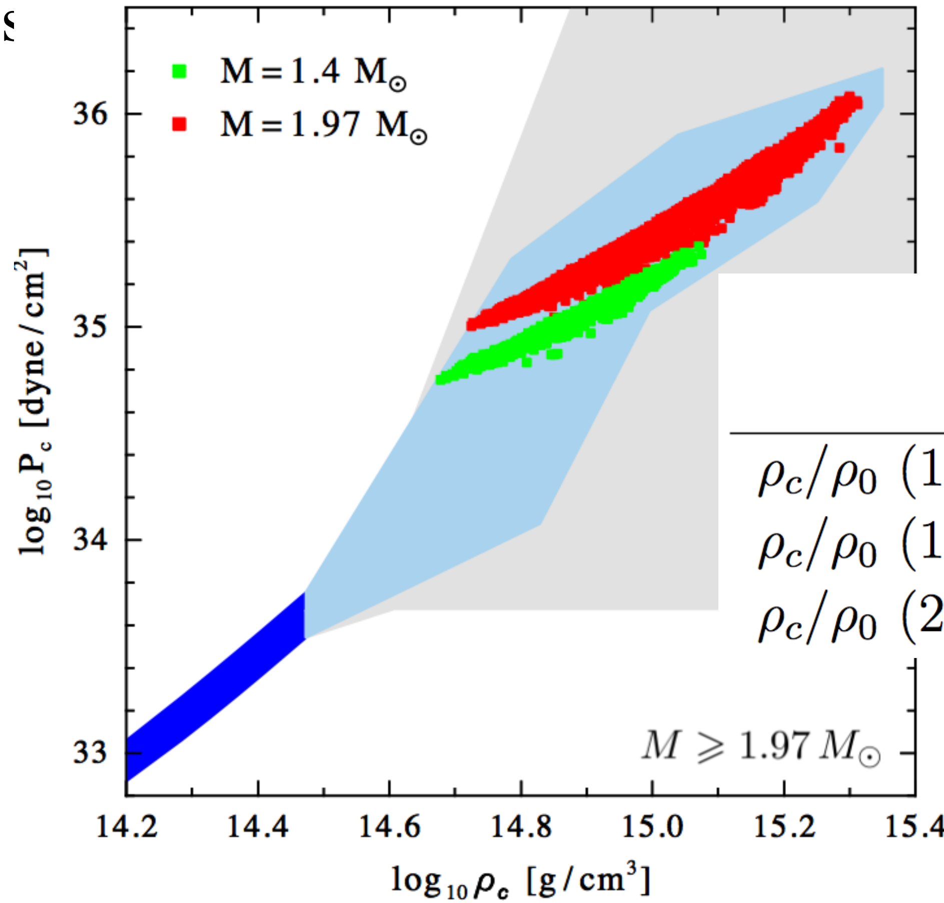

	$\widehat{M} = 1.97\, M_\odot$ min	$\widehat{M} = 1.97\, M_\odot$ max	$\widehat{M} = 2.4\, M_\odot$ min	$\widehat{M} = 2.4\, M_\odot$ max
ρ_c/ρ_0 $(1.4\, M_\odot)$	1.8	4.4	1.8	2.7
ρ_c/ρ_0 $(1.97\, M_\odot)$	2.0	7.6	2.0	3.4
ρ_c/ρ_0 $(2.4\, M_\odot)$			2.2	5.4

low-density pressure sets scale, chiral EFT interactions provide strong constraints, ruling out many model equations of state

Neutron star mergers and gravitational waves

Neutron-star mergers and gravitational waves

explore sensitivity to neutron-rich matter in neutron-star merger and gw signal

Bauswein, Janka (2012), Bauswein, Janka, Hebeler, AS (2012).

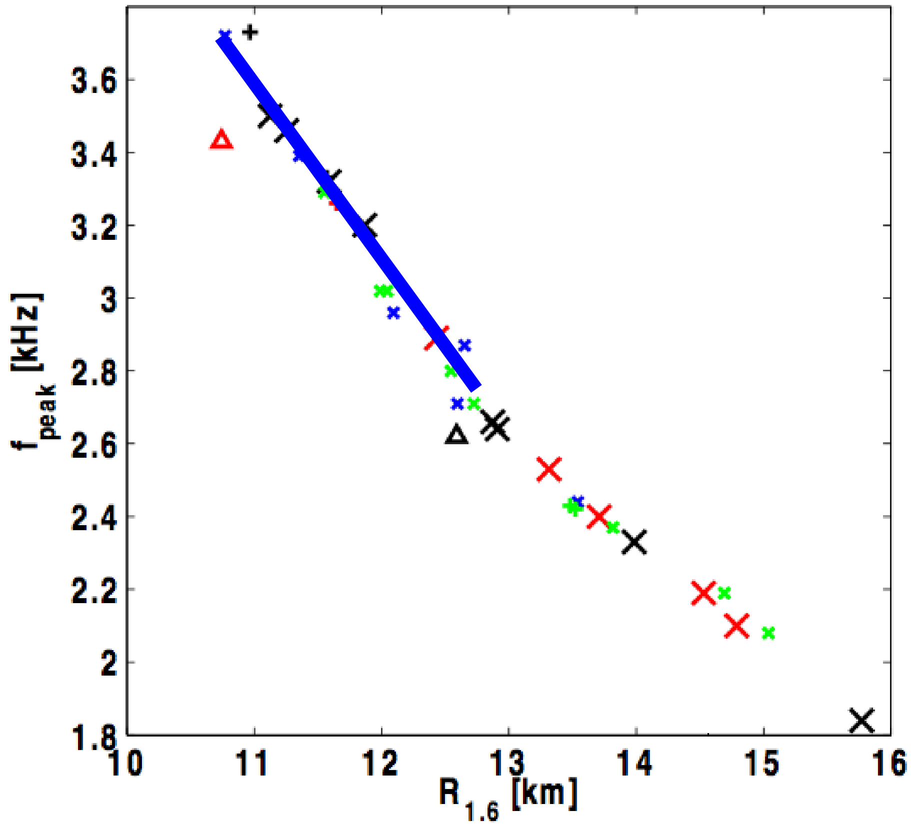

FIG. 10: Peak frequency of the postmerger GW emission versus the radius of a nonrotating NS with 1.6 $M_\odot$ for different EoSs. Symbols have the same meaning as in Fig. 8.

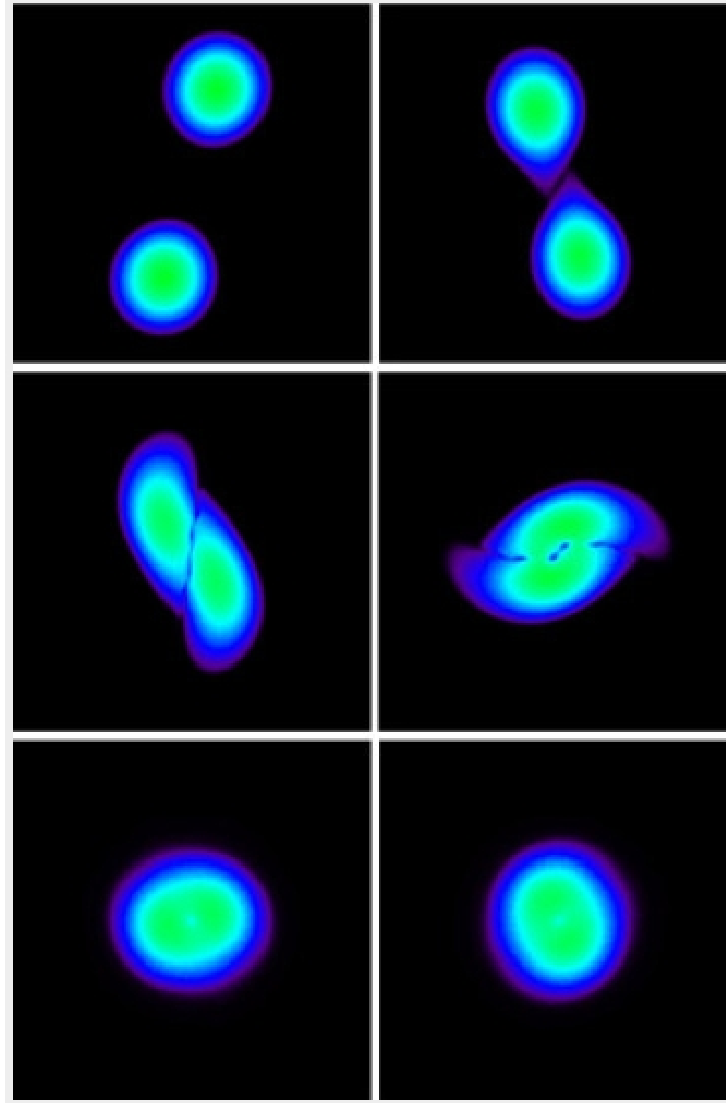

Fig. 1: Various snapshots of the collision of two neutron stars initially revolving around each other. The sequence simulated by the computer covers only 0.03 seconds. The two stars orbit each other counterclockwise (top left) and quickly come closer (top right). Finally they collide (centre left), merge (centre right), and form a dense, superheavy neutron star (bottom). Strong vibrations of the collision remnant are noticeable as deformations in east-west direction and in north-south direction (bottom panels). (Simulation: Andreas Bauswein and H.-Thomas Janka/MPA)

Direct dark matter detection

WIMP scattering off nuclei needs **nuclear structure factors** as input

particularly sensitive to nuclear physics for **spin-dependent** couplings

relevant momentum transfers ~ m_π

calculate systematically
with chiral effective field theory

Menendez, Gazit, AS (2012),
Klos, Menendez, Gazit, AS (2013)

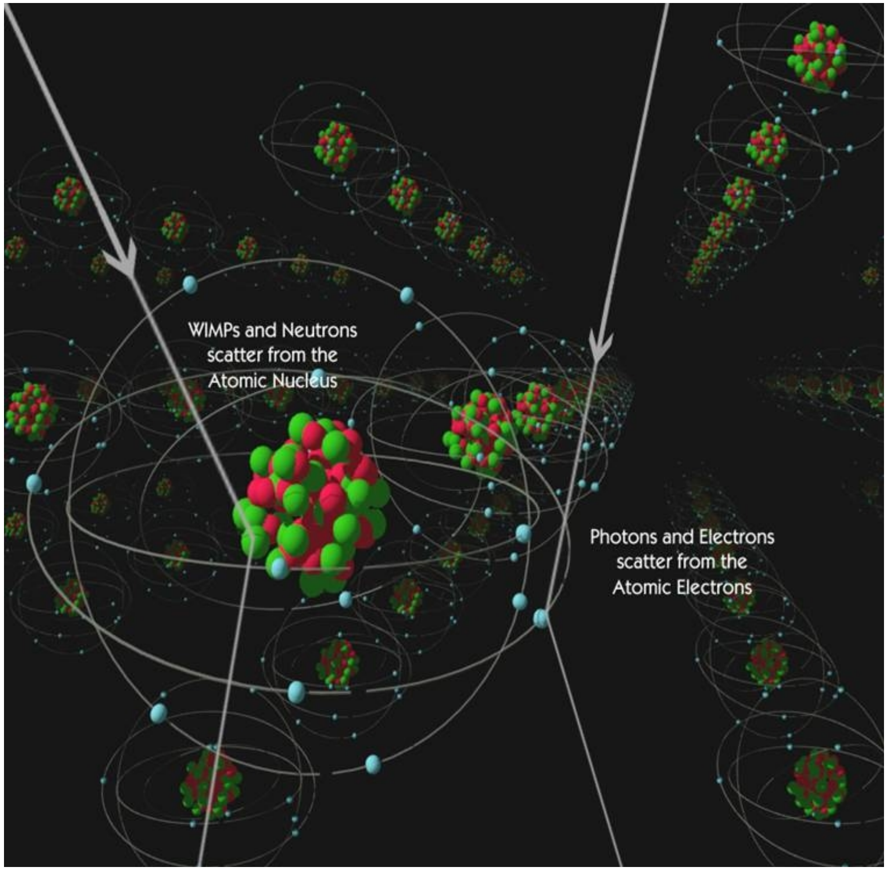

from CDMS collaboration

Chiral EFT for WIMP currents in nuclei

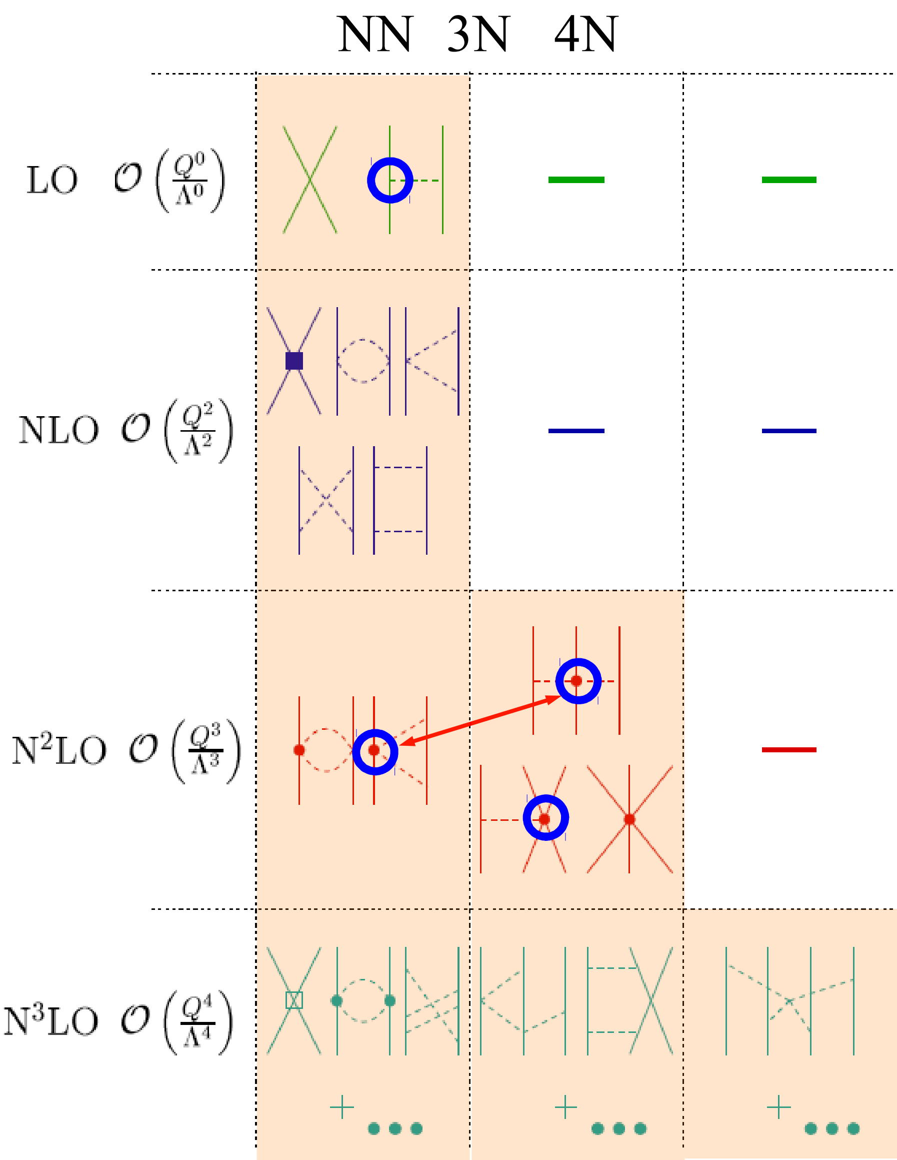

one-body currents at Q0 and Q2

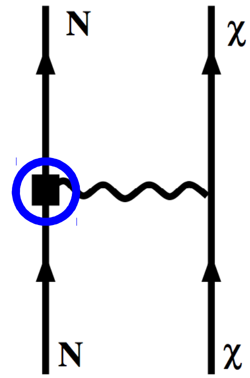

+ two-body currents at Q3

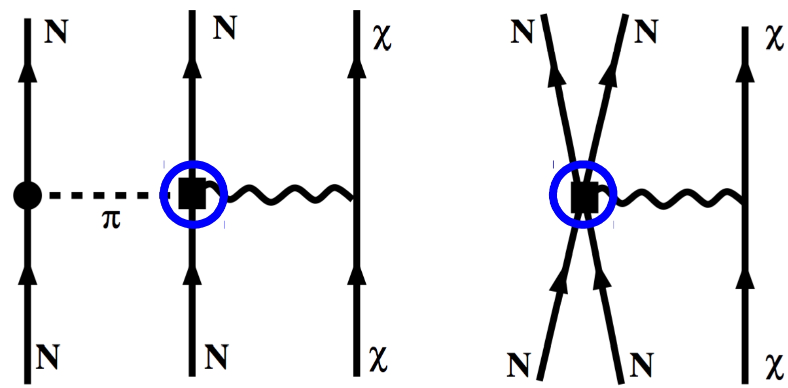

same couplings in forces and currents!

Xenon response with 1+2-body currents

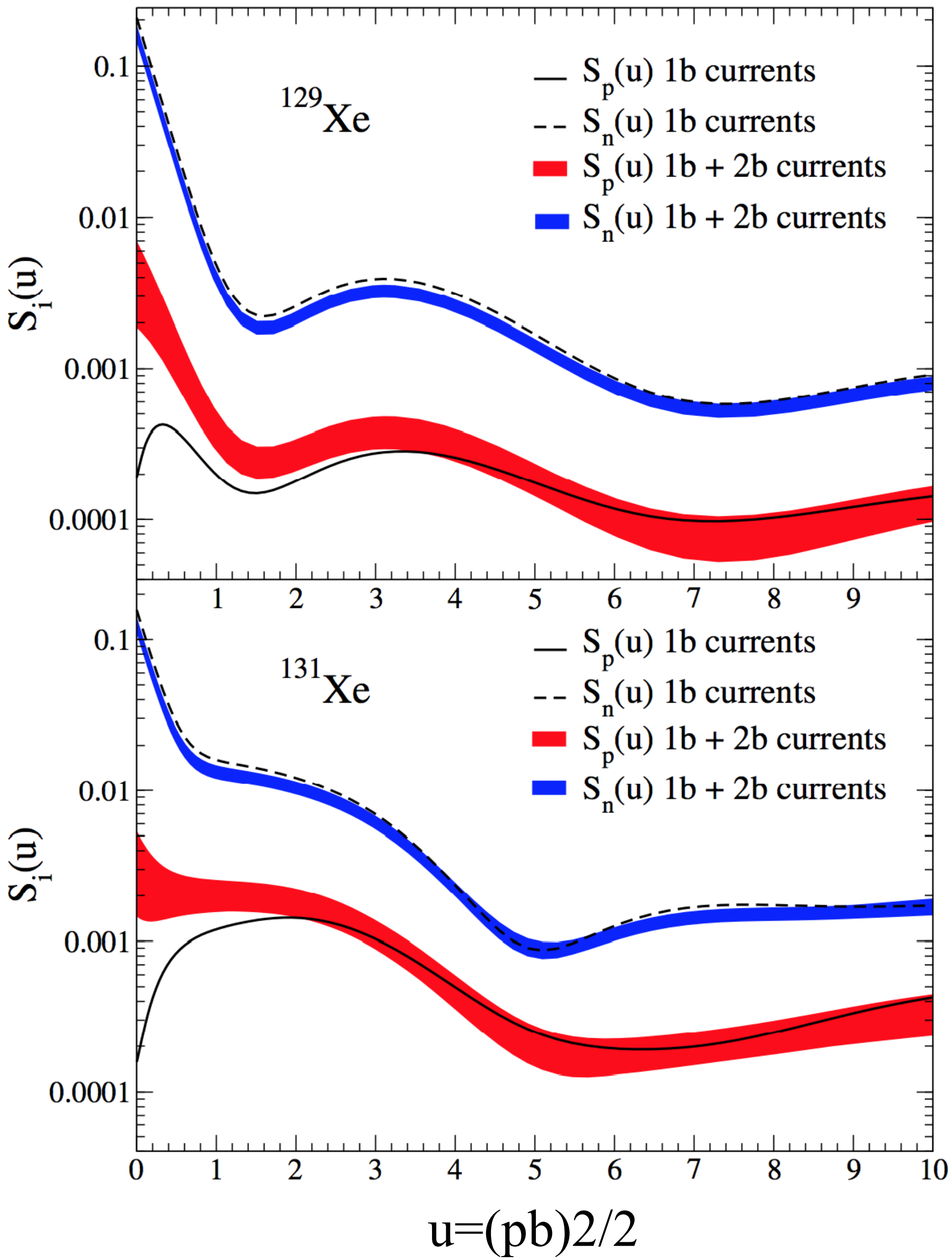

two-body currents due to strong interactions among nucleons

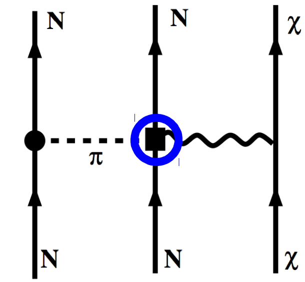

WIMPs couple to neutrons and protons at the same time

enhances coupling to even species in all cases

first calculations with chiral EFT currents and state-of-the-art nuclear interactions

Limits on SD WIMP-neutron interactions

best limits from XENON100 Aprile et al. (2013)

used our calculations with uncertainty bands for WIMP currents in nuclei

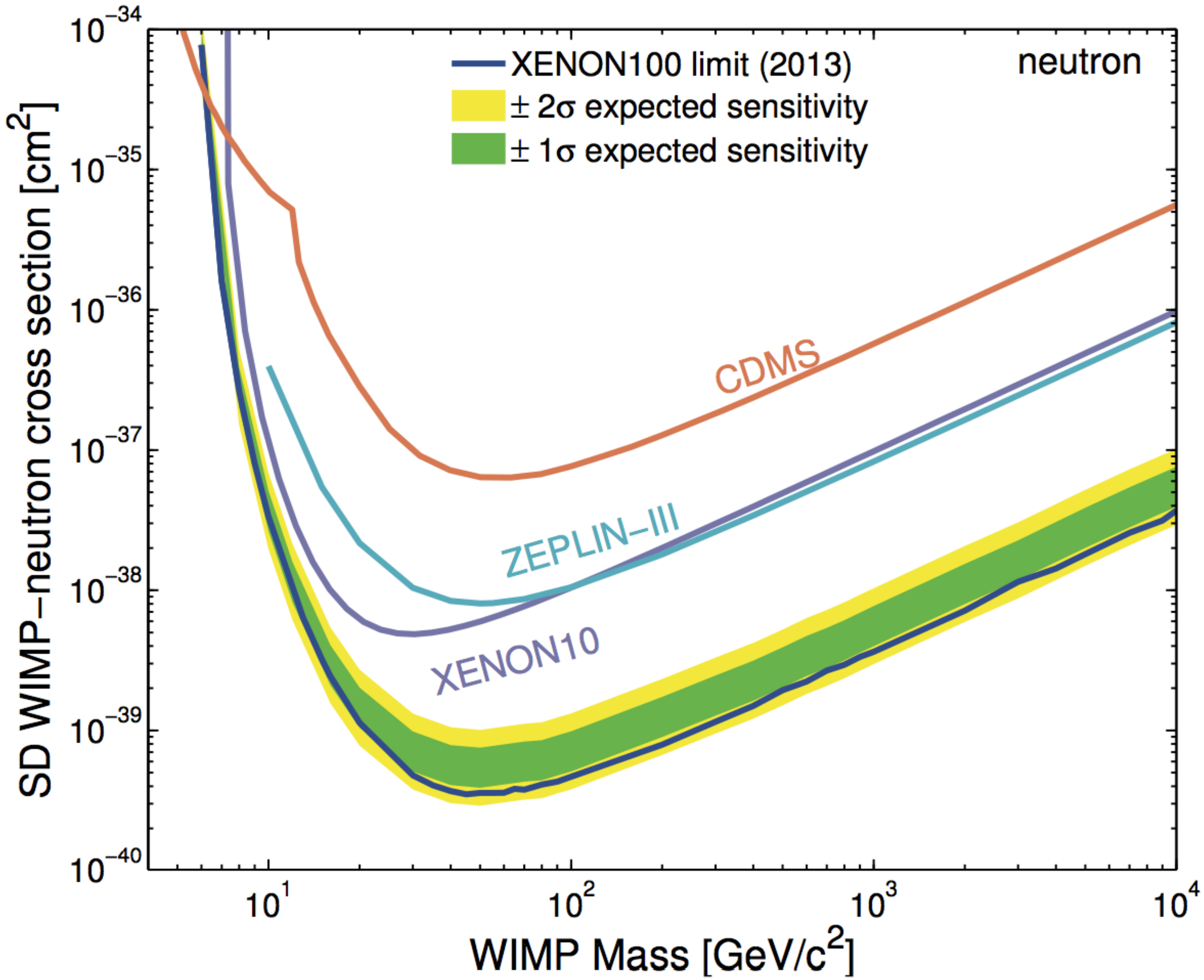

Spin-dependent WIMP-nucleus response for 19F, 23Na, 27Al, 29Si, 73Ge, 127I

Klos, Menendez, Gazit, AS (2013)

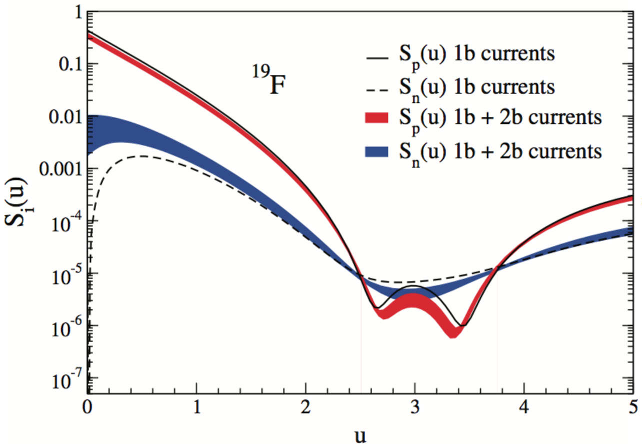

PICASSO, COUPP, SIMPLE

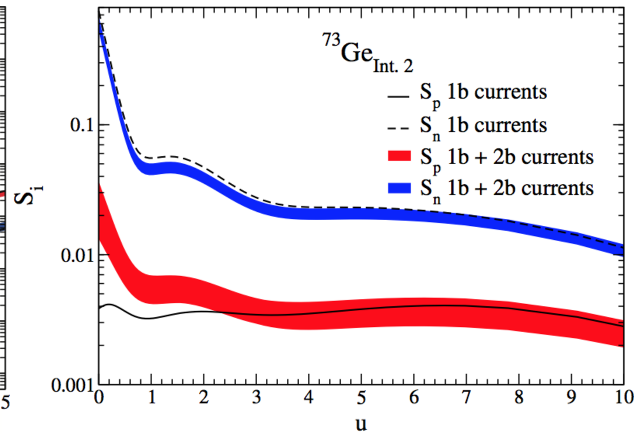

CDMS, EDELWEISS, EURECA

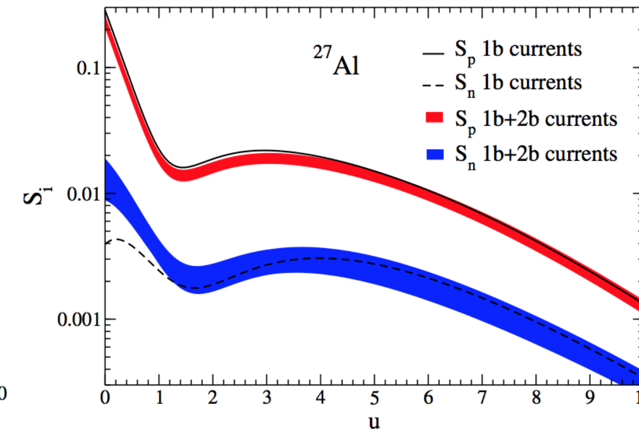

CRESST

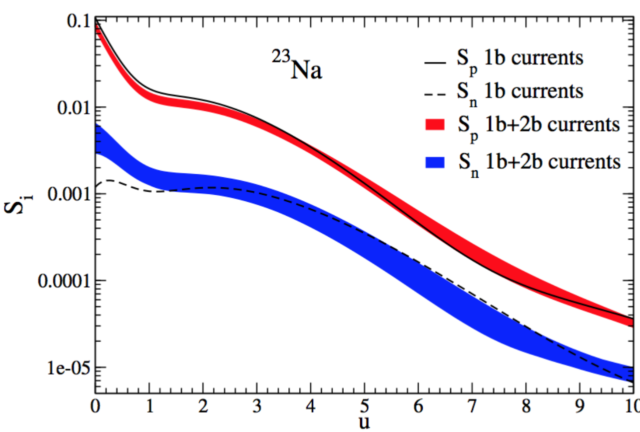

DAMA, ANAIS, DM-Ice

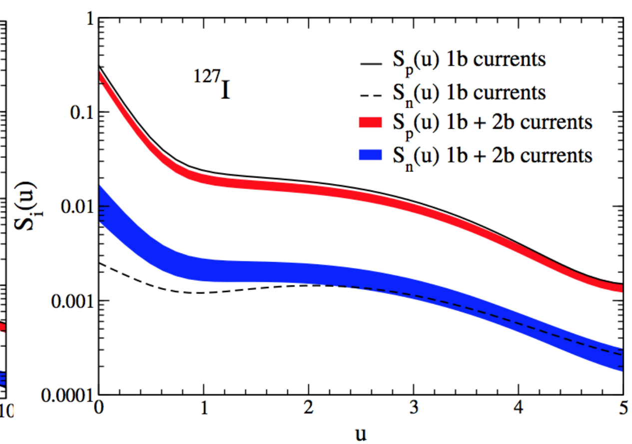

DAMA, ANAIS, DM-Ice, KIMS

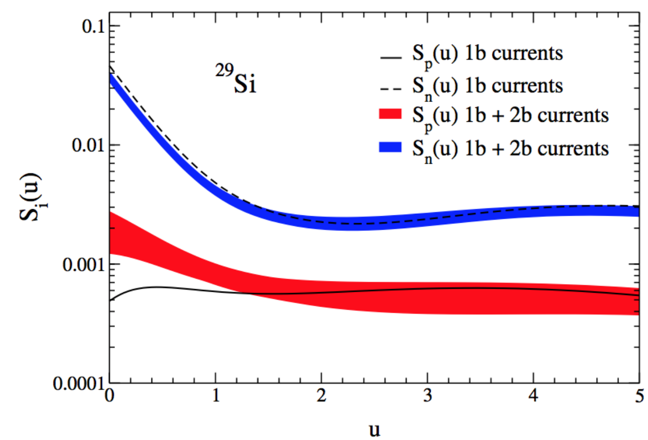

CDMS-II

Nuclear structure for direct detection

valence-shell Hamiltonian calculated from NN interactions + corrections to compensate for not including 3N forces (will improve in the future)

valence spaces and interactions have been tested successfully in nuclear structure calculations, largest spaces used

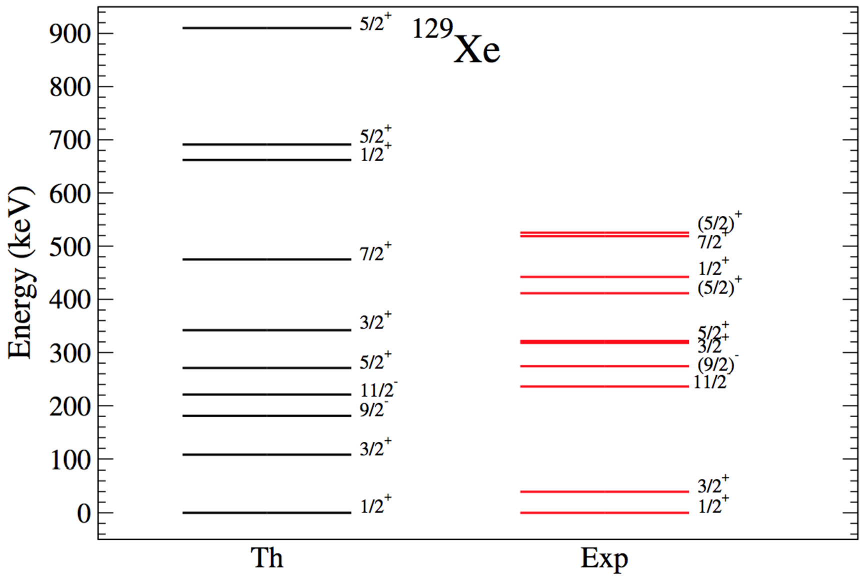

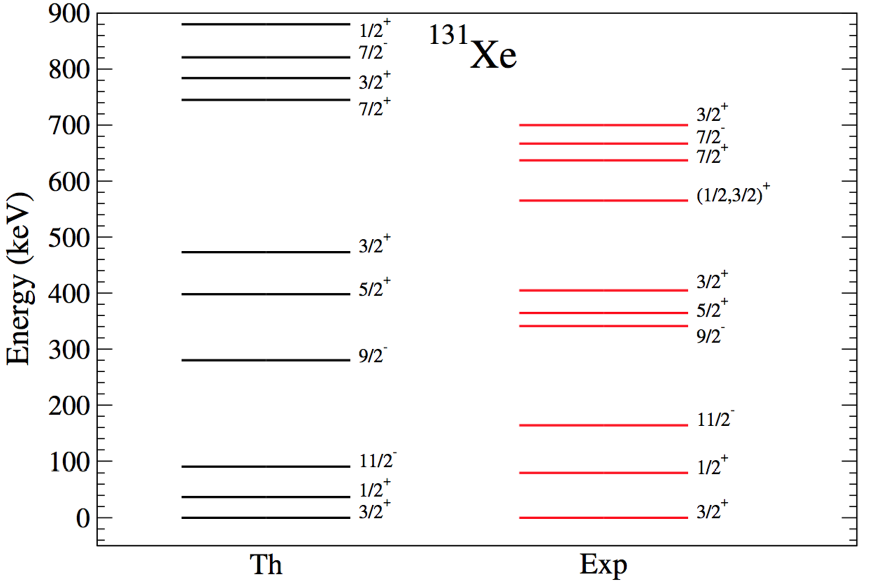

Inelastic WIMP scattering to 40 and 80 keV excited states

Baudis, Kessler, Klos, Lang, Menendez, Reichard, AS, arXiv:1309.0825

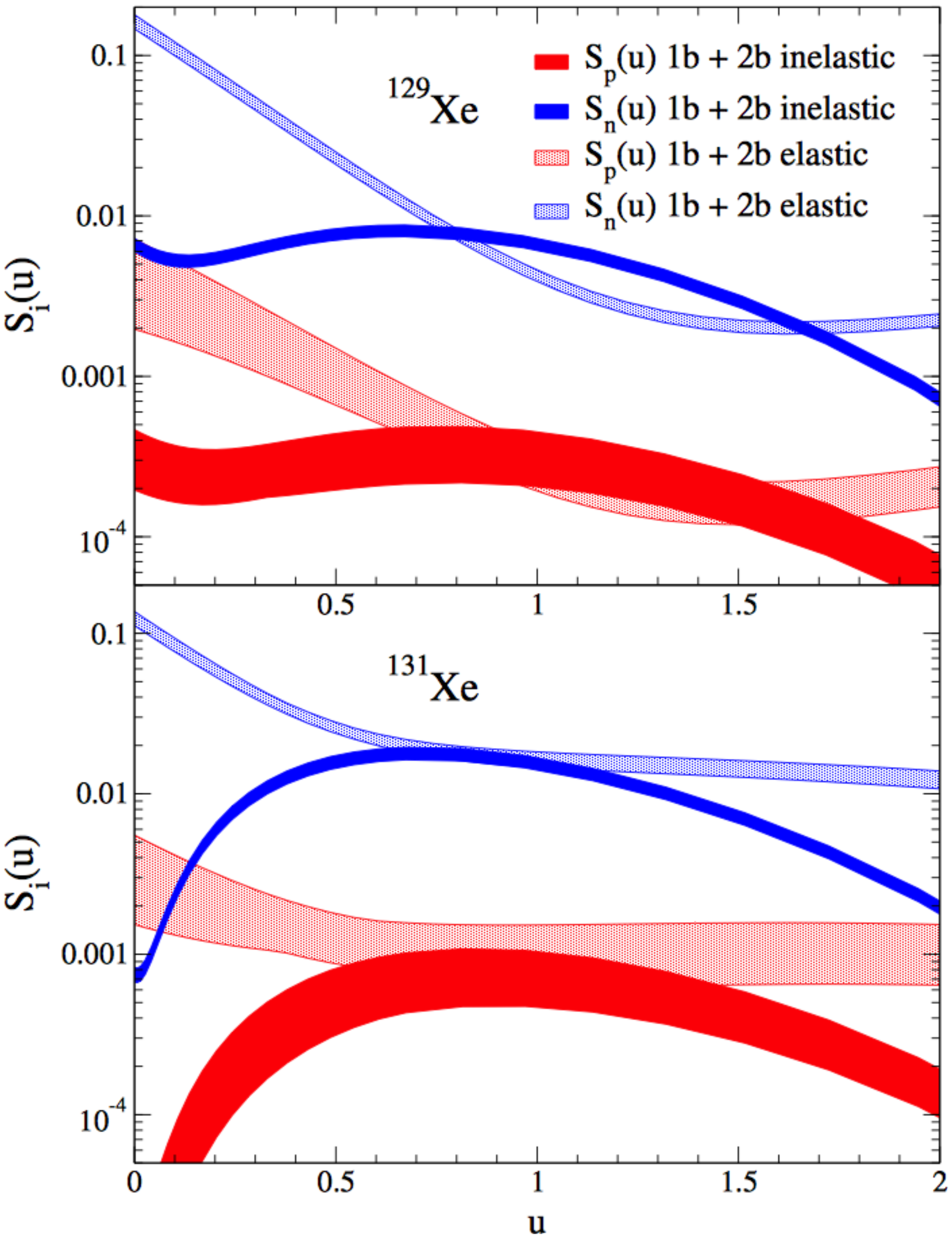

inelastic channel
comparable/dominates elastic
channel for
p ~ 150 MeV

Signatures for **inelastic** WIMP scattering

elastic recoil **+ promt γ from de-excitation**

combined information from elastic and inelastic channel will allow to **determine dominant interaction channel** in one experiment

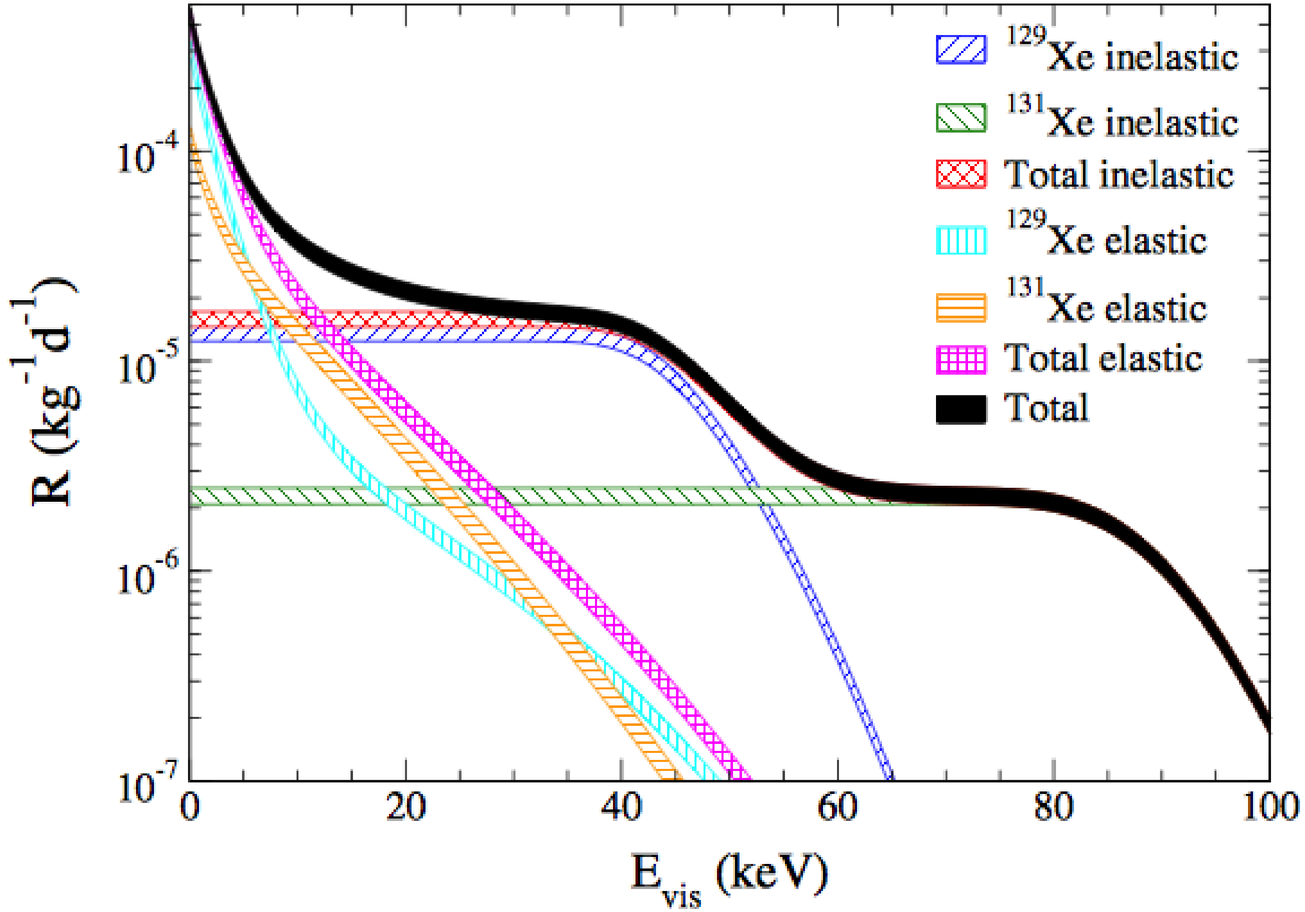

Signatures for **inelastic** WIMP scattering

elastic recoil + promt γ from de-excitation

combined information from elastic and inelastic channel will allow to **determine dominant interaction channel** in one experiment

inelastic excitation sensitive to WIMP

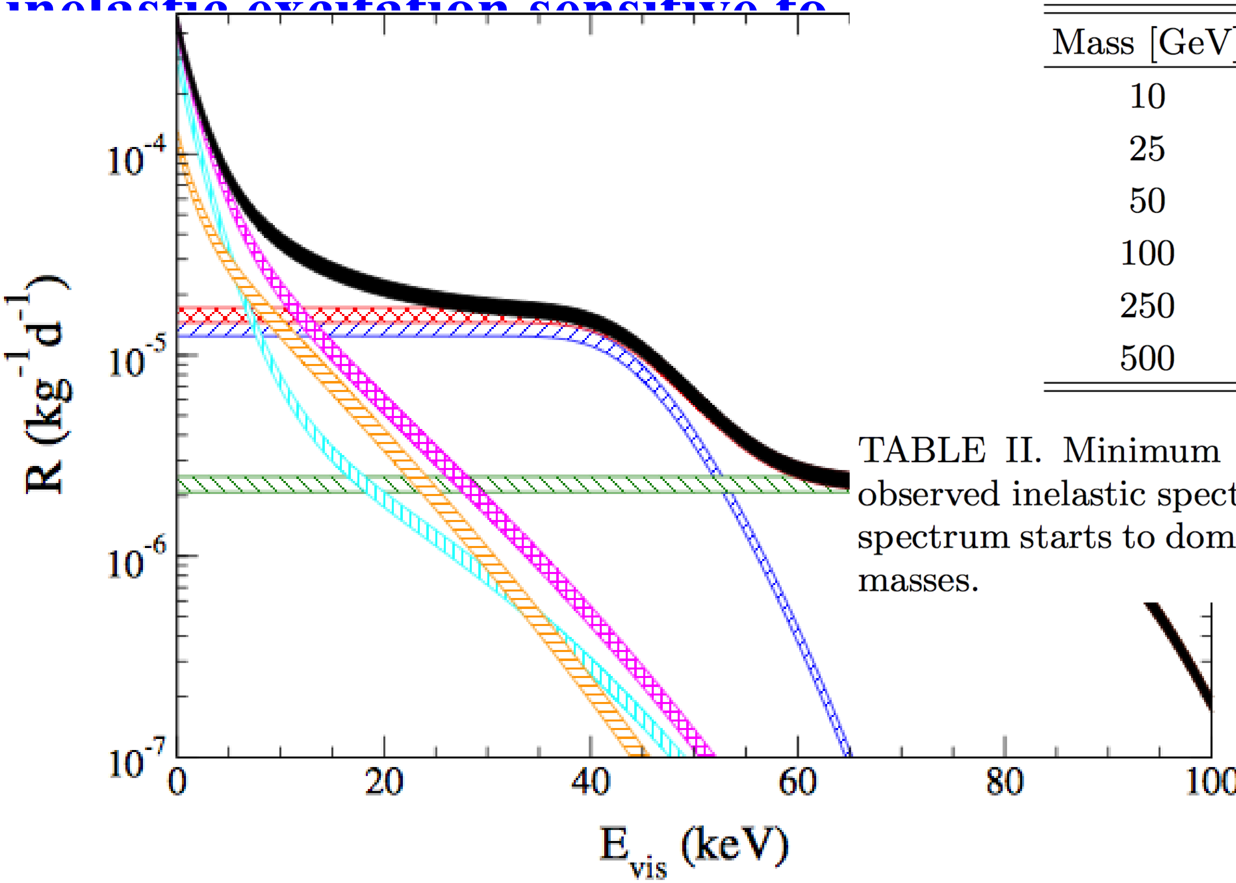

Mass [GeV]	^{129}Xe	^{131}Xe	Total
10	–	–	–
25	5	–	5
50	7	17	9
100	7	24	12
250	9	32	19
500	11	35	24

TABLE II. Minimum energy E_{vis} in keV above which the observed inelastic spectrum for ^{129}Xe, ^{131}Xe and for the total spectrum starts to dominate the elastic one for various WIMP masses.

Summary

3N forces are a frontier
in chiral EFT, for neutron-rich nuclei, matter, and neutron stars

key for **neutron-rich nuclei**: O, Ca isotopes, N=28 and shell evolution
J.D. Holt, J. Menéndez, T. Otsuka, **J. Simonis**, T. Suzuki

dominant uncertainty of **neutron (rich) matter** below nuclear densities
predicts **neutron skin** with theoretical uncertainty comparable to exp.
constrains **neutron star radii and equation of state** for astrophysics
C. Drischler, K. Hebeler, T. Krüger, V. Soma, I. Tews, J.M. Lattimer, C.J. Pethick

dark matter response of nuclei and two-body currents
J. Menéndez, P. Klos, D. Gazit

Thank you very much!

doi:10.1038/nature12226

Masses of exotic calcium isotopes pin down nuclear forces

F. Wienholtz[1], D. Beck[2], K. Blaum[3], Ch. Borgmann[3], M. Breitenfeldt[4], R. B. Cakirli[3,5], S. George[1], F. Herfurth[2], J. D. Holt[6,7], M. Kowalska[8], S. Kreim[3,8], D. Lunney[9], V. Manea[9], J. Menéndez[6,7], D. Neidherr[2], M. Rosenbusch[1], L. Schweikhard[1], A. Schwenk[7,6], J. Simonis[6,7], J. Stanja[10], R. N. Wolf[1] & K. Zuber[10]

shell gap of 4 MeV

evolution to Z=20
similar for N=28 and 32

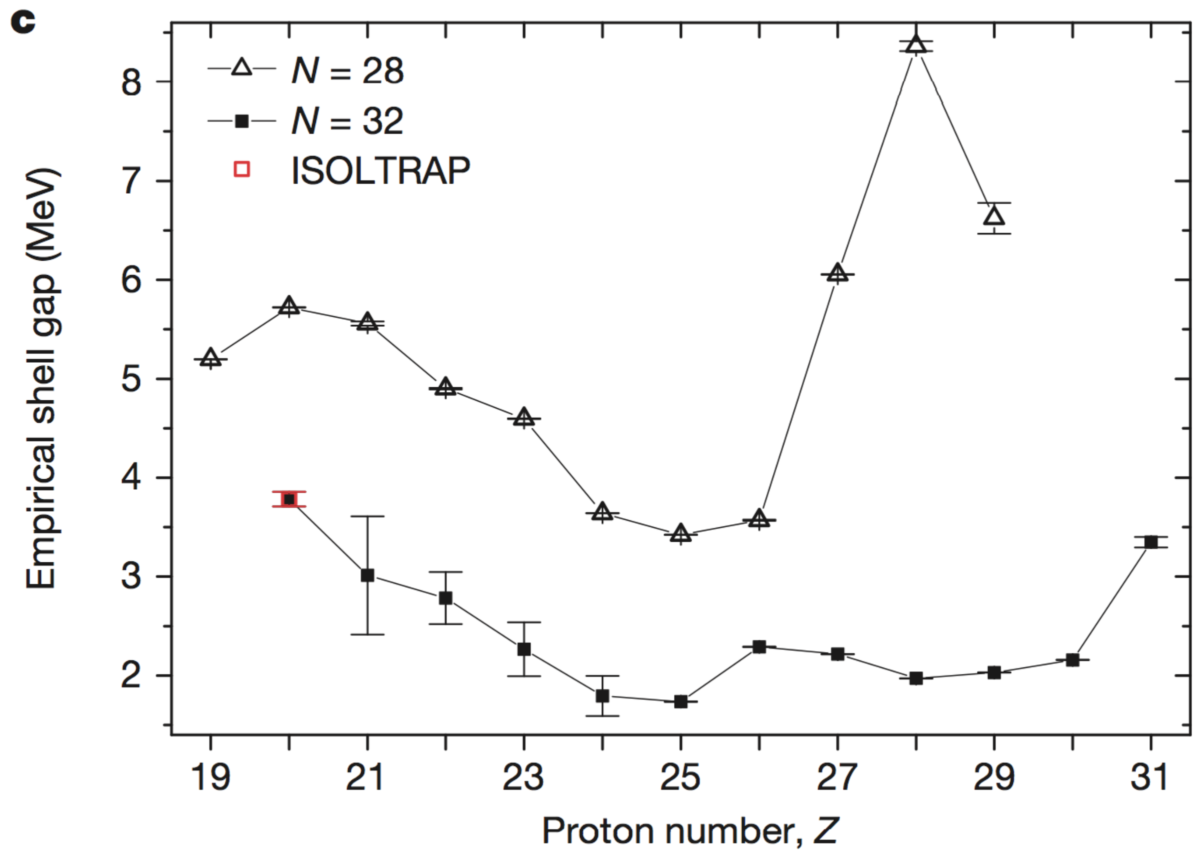

Neutron matter from chiral EFT interactions

direct calculations without RG/SRG evolution, 3N to N2LO only

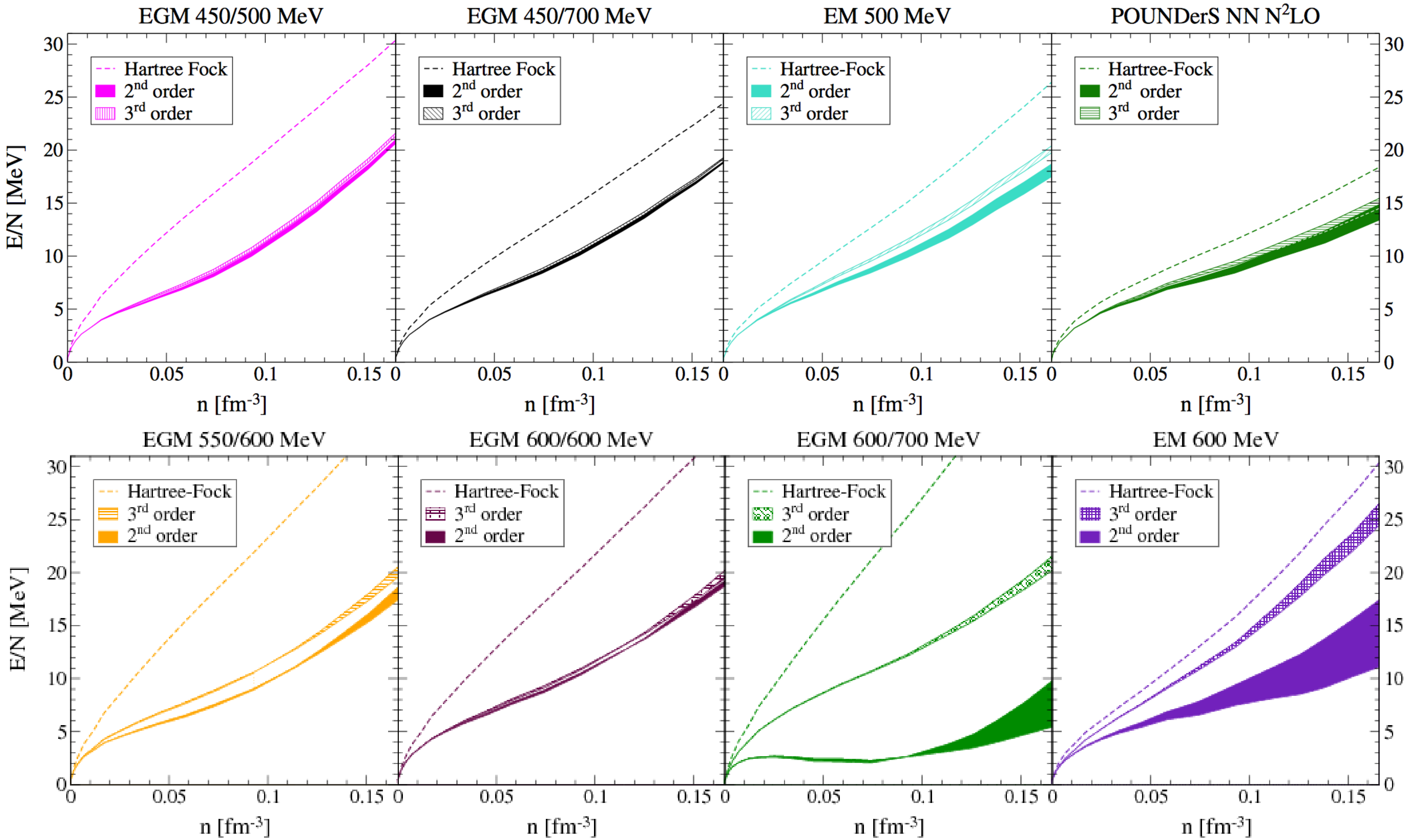

N3LO 3N and 4N interactions in neutron matter

evaluated at Hartree-Fock level

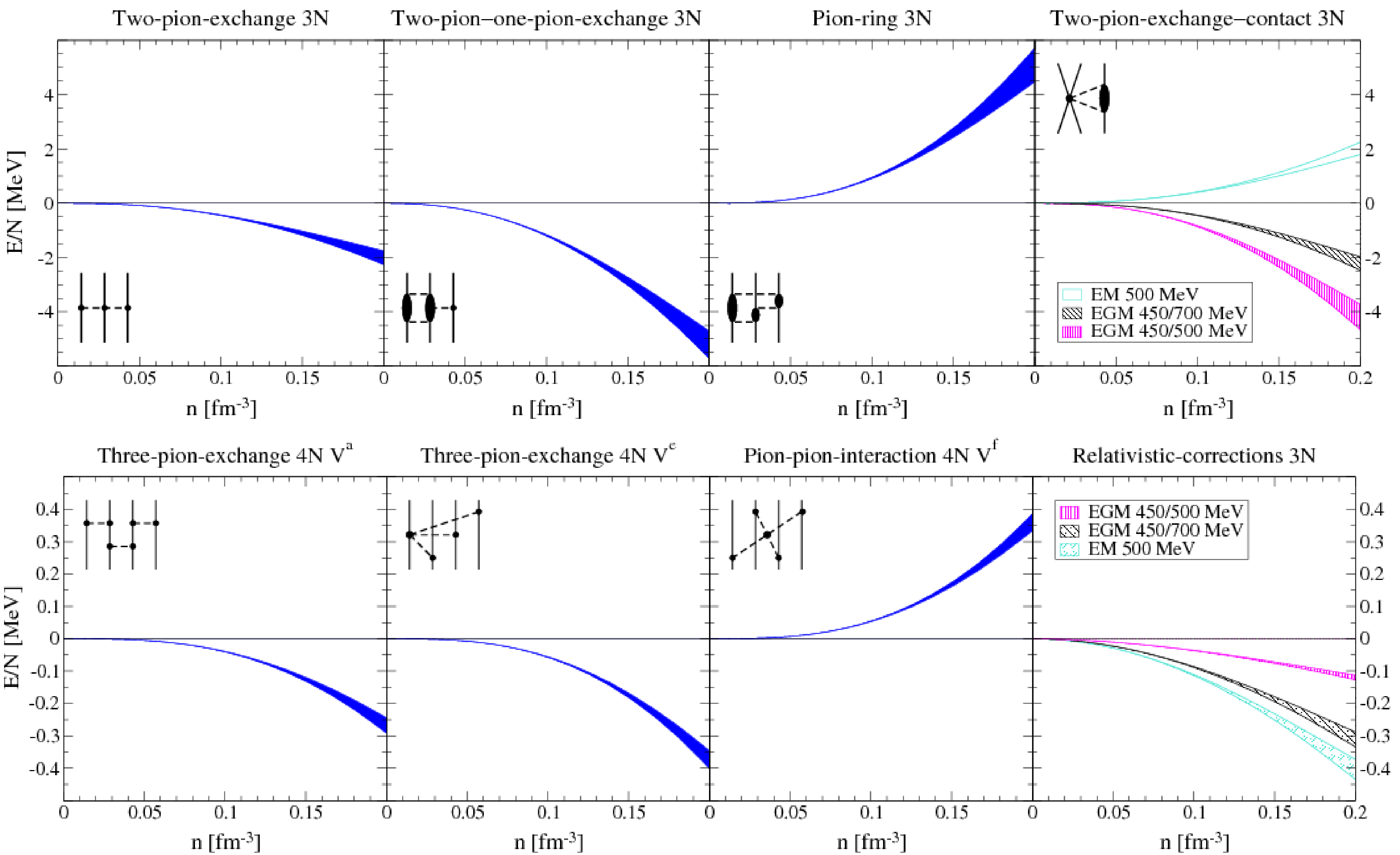

Comparisons to equations of state in astrophysics

many equations of state used in supernova simulations not consistent with neutron matter results

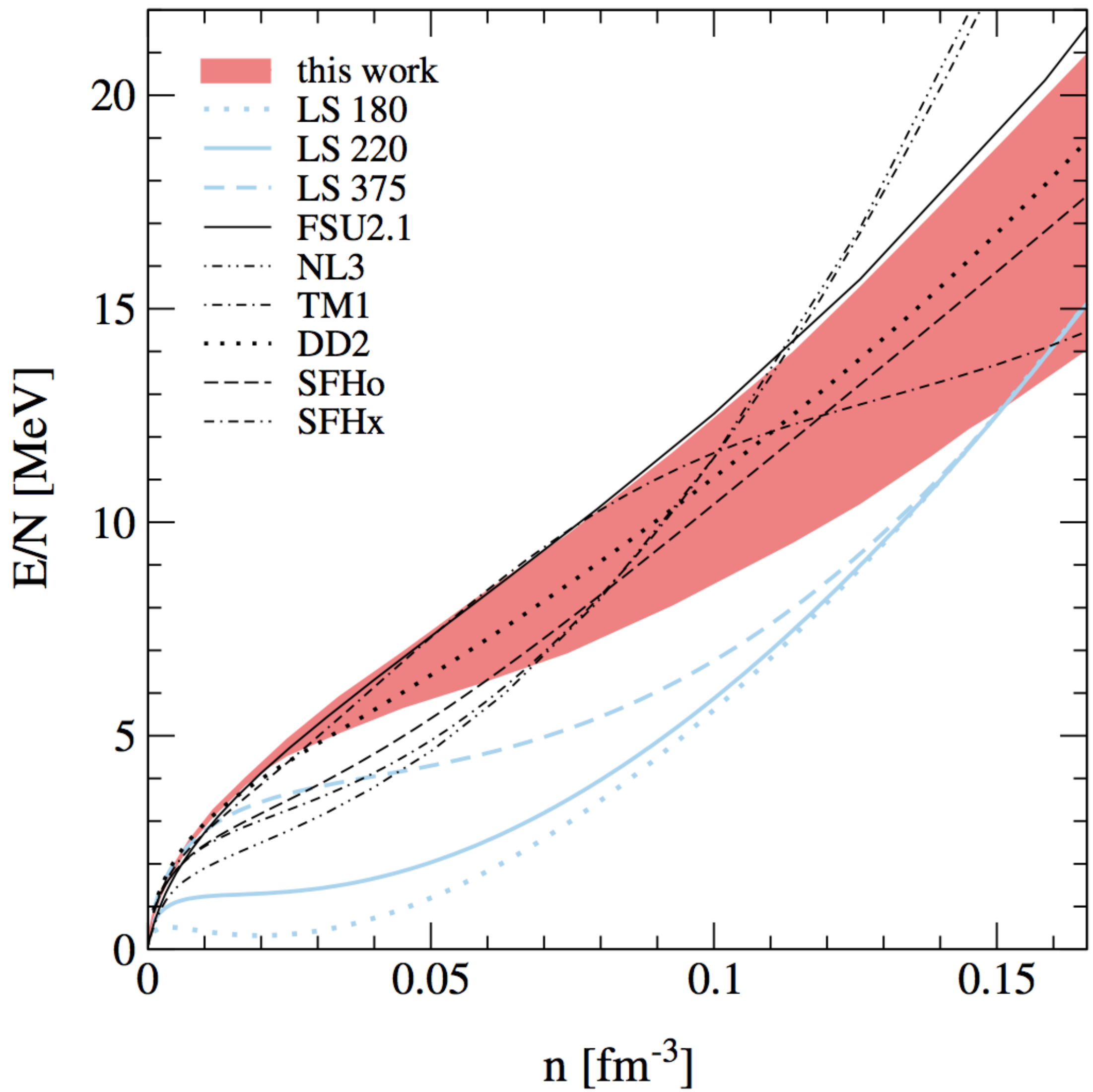

Symmetry energy and density derivative L

extract using empirical parametrization Hebeler, Lattimer, Pethick, AS (2013)

$$\frac{E(\overline{n},x)}{A} = T_0\left[\frac{3}{5}\left(x^{\frac{5}{3}}+(1-x)^{\frac{5}{3}}\right)(2\overline{n})^{\frac{2}{3}} - \left((2\alpha-4\alpha_L)\,x\,(1-x)+\alpha_L\right)\overline{n} + \left((2\eta-4\eta_L)\,x\,(1-x)+\eta_L\right)\overline{n}^{\gamma}\right]$$

expansion in Fermi momentum (γ=4/3),
kinetic energy + quadratic asymmetry

α, η fit to empirical saturation point
αL, ηL fit to neutron matter calculations

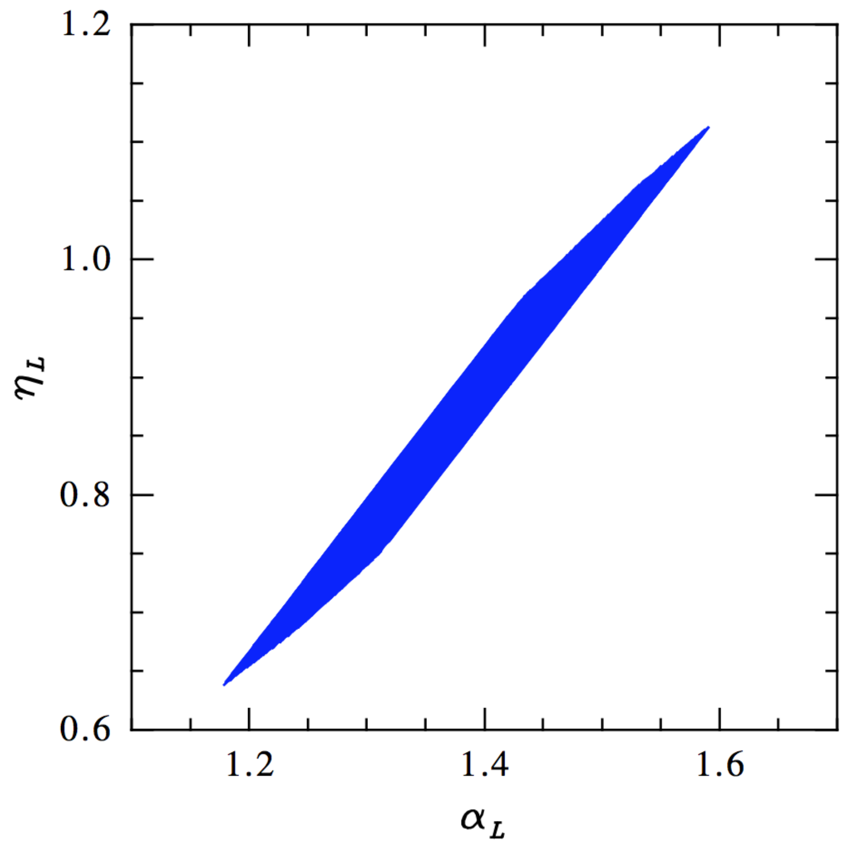

Ab-initio calculations of asymmetric matter

based on N3LO NN + N2LO 3N interactions Drischler, Soma, AS (2013)

uncertainty band dominated by 3N

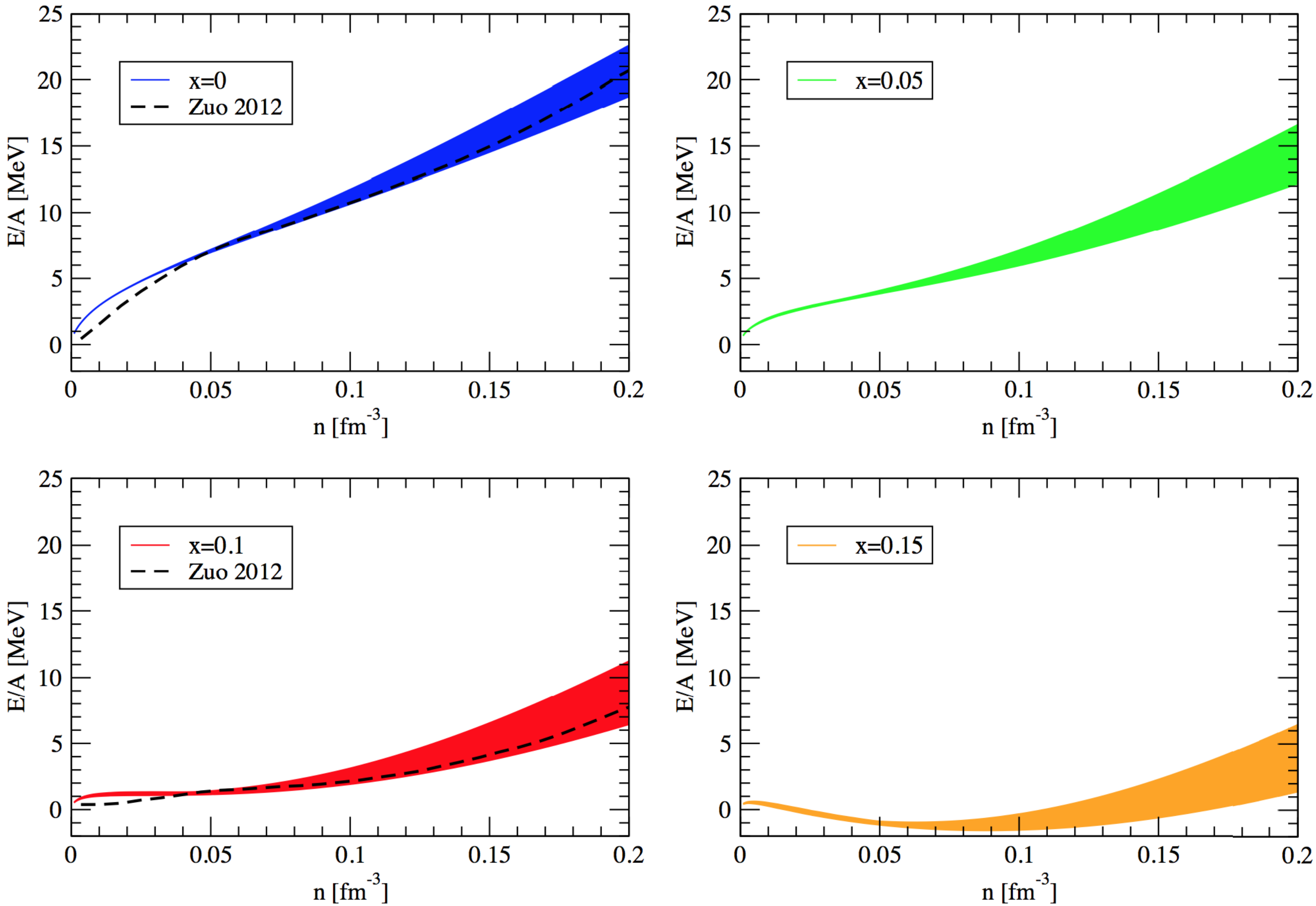

Ab-initio calculations of asymmetric matter

compares well with quadratic expansion even for n-rich conditions

$$\frac{E(n,\beta)}{A} = \frac{E(n,\beta=0)}{A} + E_{\rm sym}(n)\,\beta^2 + \mathcal{O}(\beta^4)$$

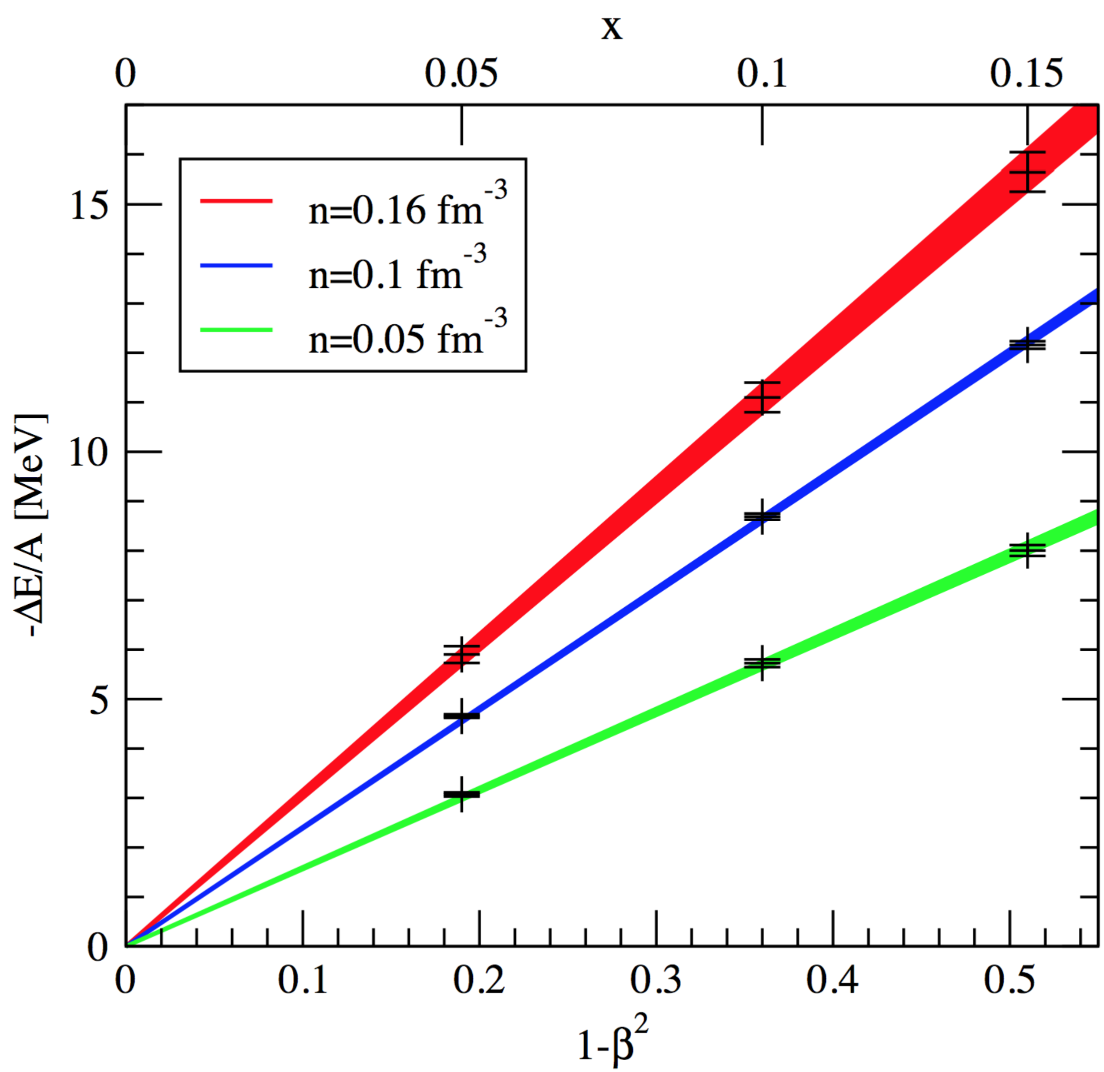

Ab-initio calculations of asymmetric matter

benchmark empirical parametrization: ΔE = diff. to neutron matter
good agreement with ab-initio calculations, very useful for astrophysics

$$\frac{E(\overline{n},x)}{A} = T_0\Bigg[\frac{3}{5}\left(x^{\frac{5}{3}} + (1-x)^{\frac{5}{3}}\right)(2\overline{n})^{\frac{2}{3}} - \left((2\alpha - 4\alpha_L)\,x\,(1-x) + \alpha_L\right)\overline{n} + \left((2\eta - 4\eta_L)\,x\,(1-x) + \eta_L\right)\overline{n}^{\gamma}\Bigg]$$

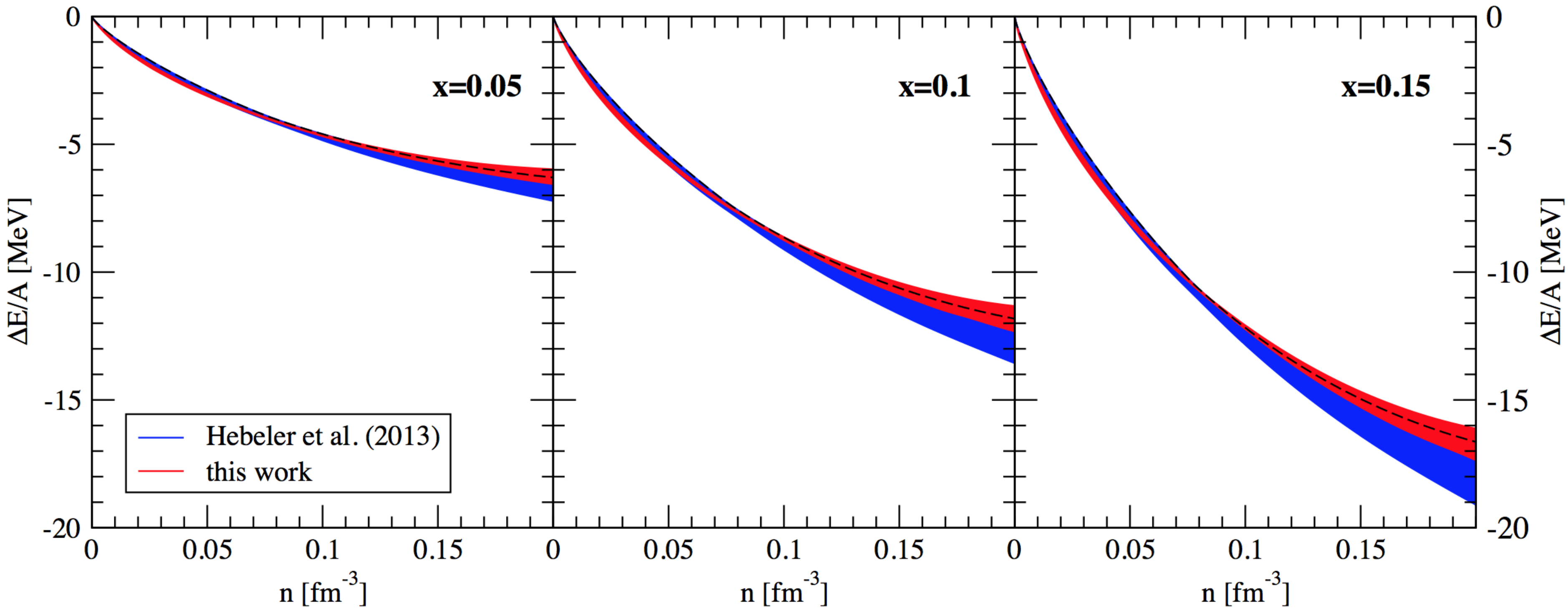

Chiral EFT currents and electroweak interactions

predicts consistent 1- and 2-body currents

GFMC calculations of magnetic moments in light nuclei Pastore et al. (2012)

2-body currents (meson-exchange currents) are key!

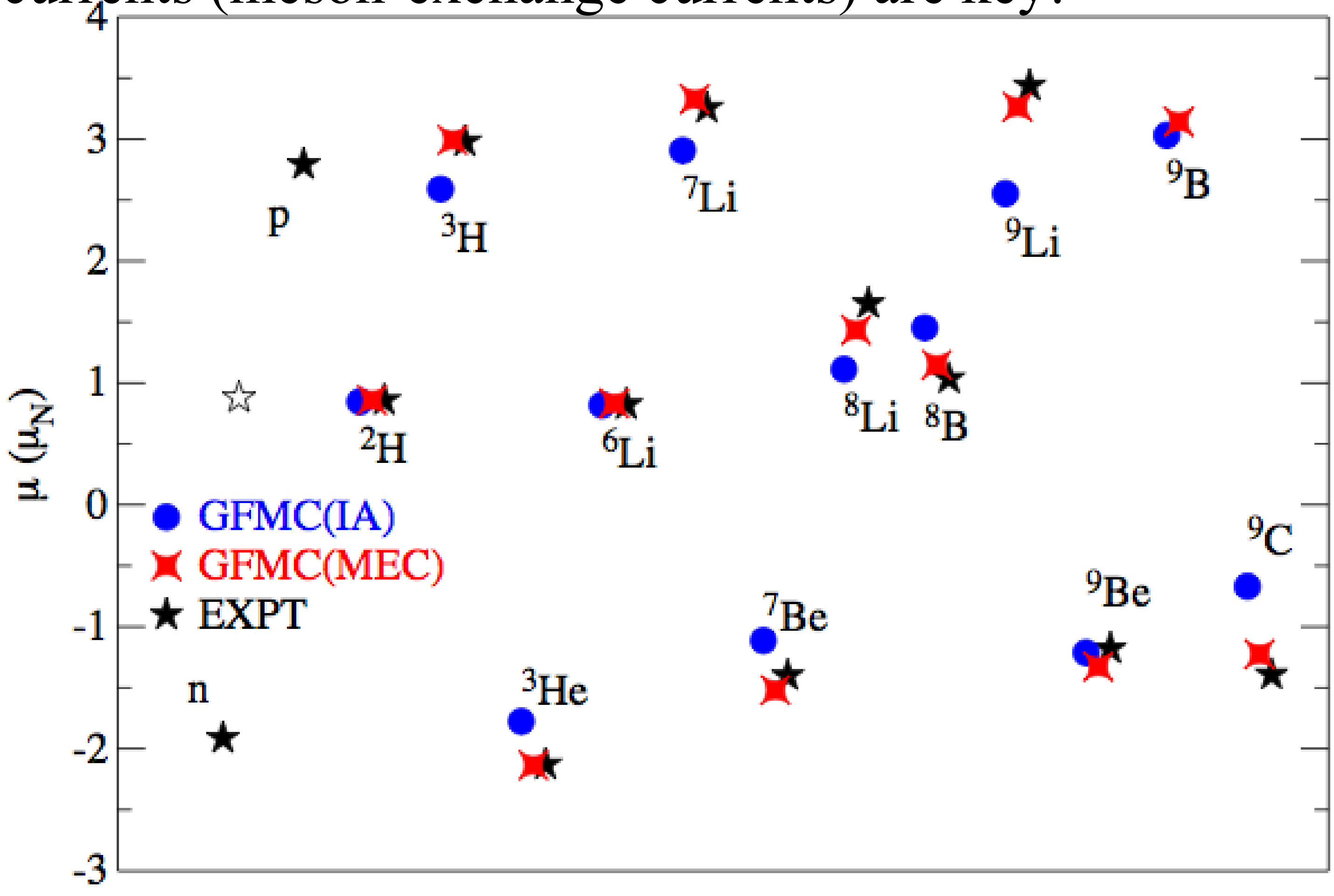

Electroweak interactions and 3N forces

weak axial currents couple to spin, similar to pions

two-body currents predicted by NN, 3N couplings to N3LO

Park et al., Phillips,…

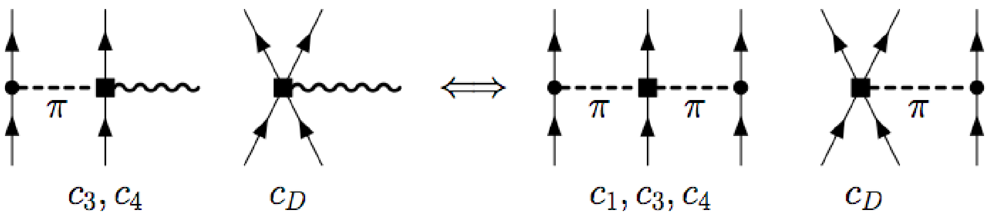

two-body analogue of Goldberger-Treiman relation

explored in light nuclei, but not for larger systems

dominant contribution to Gamow-Teller transitions,
important in nuclei (Q~100 MeV)

3N couplings predict quenching of gA (dominated by long-range part)
and predict momentum dependence (weaker quenching for larger p)

Menendez, Gazit, AS (2011)

AFDMC results for neutron matter

order-by-order convergence up to saturation density

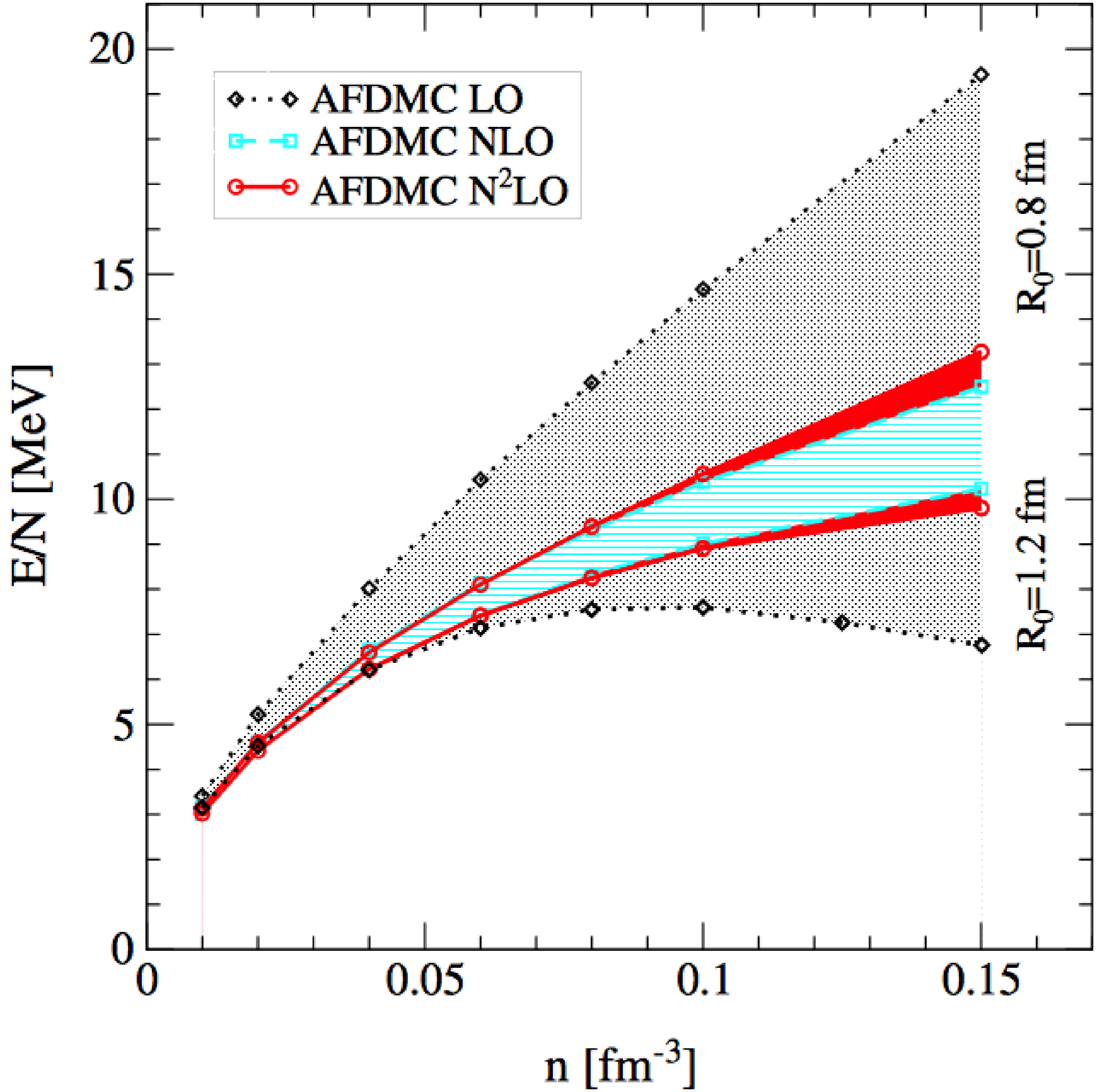

bands similar to phase shift bands

NLO ~ N2LO due to large ci

Comparison to perturbative calculations at N2LO

Hartree-Fock +2nd order +3rd order (pp+hh), same as for N3LO calcs.

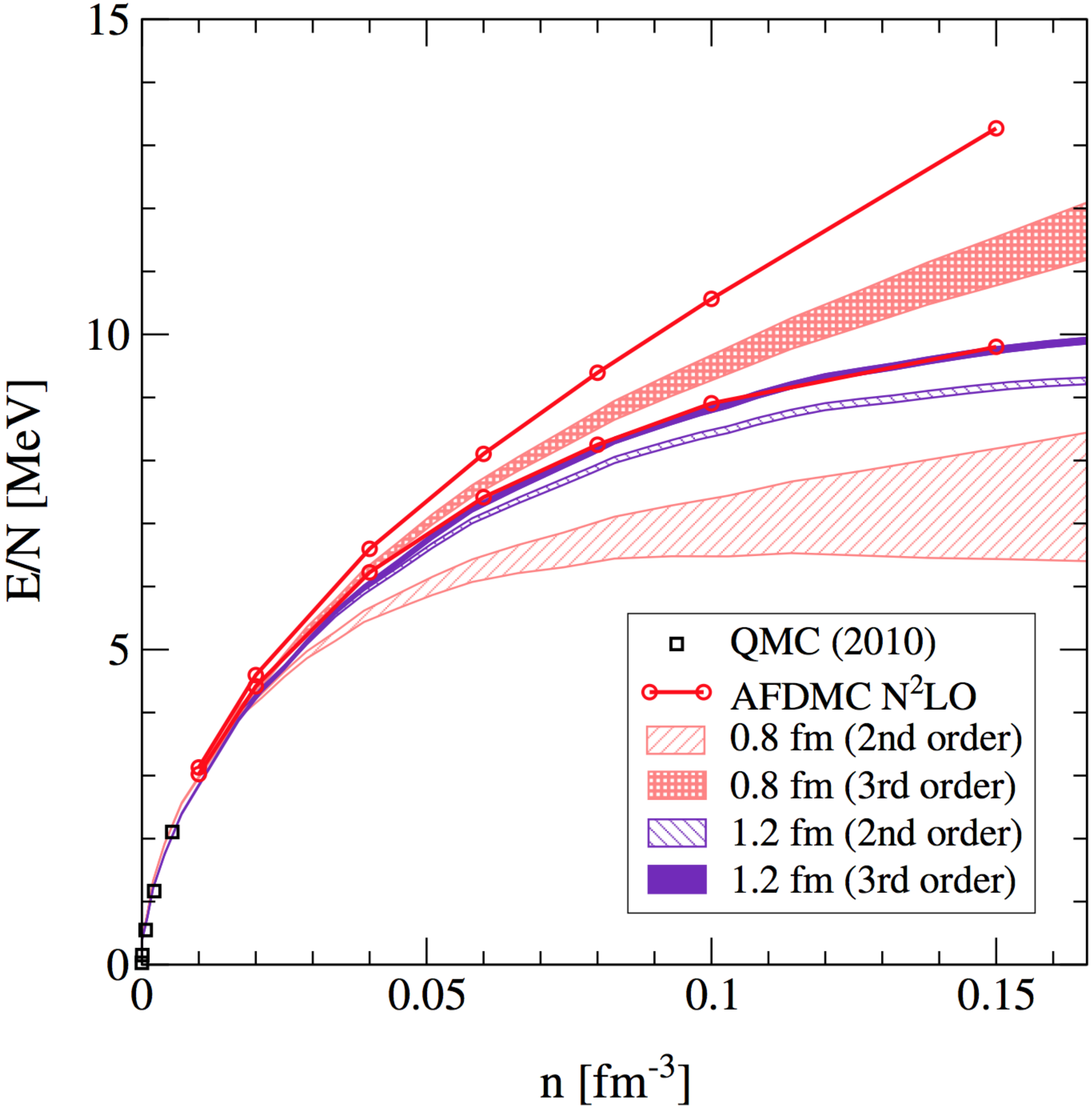

band at each order from free to HF spectrum

low cutoffs (400 MeV) 3rd order corr. small, excellent agreement with AFDMC